Chemical Engineering Journal xxx (xxxx) 134191

Contents lists available at ScienceDirect

Chemical Engineering Journal

journal homepage: www.elsevier.com/locate/cej

Synergistic effects of hybrid advanced oxidation processes (AOPs) based on hydrodynamic cavitation phenomenon – A review

Kirill Fedorov [a], Kumaravel Dinesh [a], Xun Sun [b], Reza Darvishi Cheshmeh Soltani [c], Zhaohui Wang [d,e,f], Shirish Sonawane [a,g], Grzegorz Boczkaj [a,h,*]

[a] Gdansk University of Technology, Faculty of Chemistry, Department of Process Engineering and Chemical Technology, Gdansk, Poland
[b] Key Laboratory of High Efficiency and Clean Mechanical Manufacture, Ministry of Education, National Demonstration Center for Experimental Mechanical Engineering Education at Shandong University, School of Mechanical Engineering, Shandong University, 17923, Jingshi Road, Jinan, Shandong Province 250061, PR China
[c] Department of Environmental Health Engineering, School of Health, Arak University of Medical Sciences, Arak, Iran
[d] Shanghai Key Lab for Urban Ecological Processes and Eco-Restoration, School of Ecological and Environmental Sciences, East China Normal University, Shanghai 200241, China
[e] Shanghai Engineering Research Center of Biotransformation of Organic Solid Waste, Shanghai 200241, China
[f] Technology Innovation Center for Land Spatial Eco-restoration in Metropolitan Area, Ministry of Natural Resources, 3663 N. Zhongshan Road, Shanghai 200062, China
[g] National Institute of Technology Warangal, Telangana State 506004, India
[h] EkoTech Center, Gdansk University of Technology, G. Narutowicza St. 11/12, Gdansk 80-233, Poland

ARTICLE INFO

Keywords:
Hydrodynamic cavitation
Persulfate
Oxidation
Sulfate radical
Hydroxyl radical
Wastewater treatment

ABSTRACT

High-performance water treatment systems based on cavitational processes have received an increasing interest of scientific community in the past few decades. Numerous studies indicated the advantageous application of hydrodynamic cavitation as an alternative, reagent-free treatment method of various pollutants in water. Both approaches were proved as an effective method to achieve mineralization of many organic contaminants as well as a disinfection method, which is able to eliminate pathogenic microorganisms. This makes cavitation-based methods a promising candidate implemented in a post-treatment stage of water treatment facilities. Nowadays, hybrid methods based on combination of cavitation with advanced oxidation processes (AOPs), possessing enhanced oxidation capacity were proposed. Compared to the individual utilization of cavitation and AOPs (e.g., O_3, H_2O_2, Fenton's process), hybrid processes are capable to degrade even highly persistent contaminants and shorten the operation time reducing the overall consumption of energy and oxidants. The improved performance of hybrid methods is attributed to the synergistic effect occurring between integrated technologies, which is expressed by the synergistic index. In this paper, recent reports focusing on coupling of cavitation and AOPs were reviewed to reveal major principles and mechanisms governing the synergistic effect. The review discusses the effect of process parameters (oxidant type, pH, hydraulic and ultrasonic properties, K_{ow}) on the oxidation effectiveness. Comparative analysis was provided in order to highlight the advantages and limits laying behind the discussed methods. The analysis of the economic feasibility was performed to assess the potential applicability of hybrid techniques in large-scale wastewater treatment.

1. Introduction

Continuous progress of industrialization has led to the occurrence of various emerging pollutants in water resources. Remediation of industrial wastewater containing emerging pollutants has become a critical issue that needs to be solved due to their negative impact on the public and environment. In the last decades, a great increase in the design and development of new wastewater treatment technologies took place [1-4]. Thus, a number of researches have focused on the improvement of conventional techniques by combining novel, environmentally friendly methods with higher cost effectiveness and viability. One of the most widely utilized approaches is the implementation of various treatment techniques in combination with AOPs [5,6]. In general, the preliminary and basic treatment technologies are based on physical processes (e.g., adsorption, coagulation, flocculation, sedimentation, and biofiltration), chemical (additions of chemicals), and biological means (i.e., activated

* Corresponding author at: Gdansk University of Technology, Faculty of Chemistry, Department of Process Engineering and Chemical Technology, G. Narutowicza St. 11/12, Gdansk 80233, Poland..
E-mail address: grzegorz.boczkaj@pg.edu.pl (G. Boczkaj).

https://doi.org/10.1016/j.cej.2021.134191
Received 2 July 2021; Received in revised form 27 October 2021; Accepted 13 December 2021
1385-8947/

sludge process) [7,8]. The AOPs can result in degradation and mineralization of pollutants in the aqueous phase by producing reactive species, such as hydroxyl radicals (•OH). •OH radicals with oxidation potential of 2.80 V can non-selectively attack and rapidly oxidize majority organic contaminants at rate constant in the order of 10^6-10^9 M^{-1} s^{-1} [9,10]. Recently, the application of cavitation in wastewater treatment is one of the "hot" topics [11]. Cavitation technology, which combines the features of enhanced oxidation and thermal decomposition, is a powerful and novel wastewater treatment technique for the degradation of toxic and persistent organic pollutants [11,12]. It can be used alone or in hybrid processes i.e., combination with other AOPs.

Sono- and hydrodynamic cavitation are the most studied and commonly used technologies in water treatment. Oscillation and collapse of cavities in sonocavitation are generated in the phase of acoustic wave discharge induced by US. In HC, cavitation bubbles are generated when the liquid is forced through solid constrictors (orifice plate, Venturi tube) due to a local drop of static pressure of a liquid below the critical value [13]. Short reaction time, high effectiveness, robust equipment are of benefits of HC technology in water treatment [11,14].

Recently, hydrodynamic cavitation (HC) based hybrid processes have shown a great potential in indusial scale water treatment [15,16]. Several studies revealed the synergism between HC and AOPs utilized in water and wastewater treatment [11,14,17]. For instance, combined processes of HC with AOPs improved the treatment of recalcitrant organic pollutants and endocrine disruptors [18-20]. To better understand the synergistic effect of the HC-based treatment processes, it is essential to determine the synergy index and its influence on COD and TOC removal as well as the reaction rate of particular processes. Therefore, this review focuses on critical assessment of the synergy in HC-based hybrid processes, with the following objectives: (i) to study the effect of synergy between HC-based processes and other AOPs in respect to particular external oxidants for degradation of specific types of pollutants; (ii) to study the process efficiency towards target pollutants, including total mineralization effectiveness characterized by COD and TOC removal; (iii) to determine the rate constants of hybrid techniques and to define the general rules driving the synergism and its typical range of values.

2. Synergistic effect of HC and ozone

Ozone (O_3) has low water stability and solubility and reacts selectively with organic compounds at acidic pH. In addition, O_3 slowly responds to specific organic compounds (e.g., saturated carboxylic acids or inactivated aromatics), and in many instances does not degrade and mineralize aforementioned organic compounds completely [9,21]. These disadvantages limit the use of O_3 in industrial scale wastewater treatment.

Ozone interacts with organic compounds in molecular state in both acidic and neutral pH [22-24]. When O_3 is used in alkaline conditions, it is easily decomposed and generate highly reactive radicals mainly •OH. Thus, HC/O_3 conducted at basic pH is able to degrade effectively persistent organic pollutants. Cavitation in aqueous solution results in formation and adiabatic collapse of microbubbles. Collapse of microbubbles generates localized regions with extreme conditions (5000 K, 1000 atm) 'hot-spots'. Due to pyrolysis and radical reactions taking place at the gas phase, organic compounds can be degraded within the bubble interior. Radicals that diffuse from the collapsing cavitation bubble can further react at the gas liquid interface with the pollutants remaining in the liquid phase. In case of HC/O_3, O_3 decomposition within bubbles generates an increased amount of •OH. In addition, turbulent flowrate that takes place in the cavitation region which increases the mass transfer of O_3 [17,25]. A well-known limiting stage of ozonation is the mass transfer of O_3 molecules in the treated liquid. Application of HC causes high overpressure before the constriction enhancing O_3 absorption. Furthermore, cavitation accelerates O_3 decomposition, resulting in the maximized generation of •OH. Studies on combining HC and O_3 reported the main advantages of hybrid process as: (i) reduced reaction time, (ii) improved degradation efficiency, and finally (iii) synergy. The synergistic index (ξ) of the hybrid process can be determined by comparing the rate constant of sole processes (k_{Cav}, k_{AOPs}) with the rate constant of the combined process ($k_{Cav/AOPs}$):

$$\xi = \frac{k_{Cav/AOPs}}{k_{Cav} + k_{AOPs}} \quad (1)$$

Table 1 presents a summary of observations on synergism related to above mentioned aspects. It is found that the dissolution of the O_3 has higher impact onto the degradation and hence the synergistic effect. Above pressure of 4 bar the cavitating conditions are highly fa-

Table 1
Recent studies on the wastewater treatment by combining HC and O_3.

Treated compound/wastewater	Conc. (mgL^{-1})	ξ	Process conditions	k (min^{-1})	Efficiency/contact time, (%/min)	Ref.
4-chloro-2-aminophenol	20	1.01	Inlet pressure 4 bar O_3 flow rate 0.4 gh^{-1} pH 6	1.15×10^{-2}	73.4/120	[26]
Tannery waste effluent	8800–10080	1.13	Inlet pressure 5 bar O_3: 7 gh^{-1}pH ~ 7	3.3×10^{-3}	COD 26.8/120	[27]
Effluent of bitumen production	11,020	1.20	Inlet pressure 8 bar O_3: 9.4 gh^{-1} pH 10.5	–	COD 39.7/360	[14]
Triazophos	20	1.28	Inlet pressure 5 bar O_3: 1.95 gh^{-1} pH 3	60.98×10^{-3}	TOC 96/90	[28]
Industrial effluent	20,800	1.30	Inlet pressure 4 bar O_3 flow rate 2 gh^{-1} pH 4	6.5×10^{-3}	COD 52.8/120	[29]
Textile dyeing effluent	556–1184	1.42	Inlet pressure 5 bar O_3: 3 gh^{-1} pH 6.8	6.4×10^{-3}	TOC 48/120	[30]
2,4,6-trichlorophenol	20	1.48	Inlet pressure 4 bar O_3: 0.4 gh^{-1} pH 7	2.87×10^{-2}	TOC 94.4/120	[31]
Potassium thiocyanate	20	1.55	Inlet pressure 4 bar O_3: 0.4 gh^{-1} pH 2	17.2×10^{-3}	71/120	[32]
Phenol	94	1.55	Inlet pressure 7 bar O_3: 0.2 gh^{-1} pH 5.2	28×10^{-3}	80/30	[33]
Rhodamine 6G	50	1.58	Inlet pressure 5 bar O_3: 3 gh^{-1} pH 10	10.9×10^{-3}	TOC 73.2/120	[34]
Pesticide effluent	17000–18000	1.80	Inlet pressure 6 bar O_3: 0.75 gh^{-1} pH 7	2.47×10^{-3}	COD 25.7/120	[35]
Brilliant Cresyl Blue dye	5	1.84	Inlet pressure 1.7 bar O_3: 64.3 g/h pH 7	9.9×10^{-1}	COD 97/1	[36]
2,2-dichlorovinyl dimethyl phosphate	50	2.10	Inlet pressure 5 bar O_3: 0.4 gh^{-1} pH 4	17.8×10^{-3}	TOC 39.4/120	[37]
Kitchen greywater	354.7–549.2	2.84	Inlet pressure 5 bar O_3: 3 gh^{-1} pH 3	7.1×10^{-3}	TOC 35/60	[38]
Naproxen	10	12.3	Inlet pressure 4 bar O_3: 2 gh^{-1} pH 3	0.15	100/40	[39]

vorable for dissolution of O_3 and generating the radicals. There is also dependency on the presence of the hydrophobic components present in the wastewater. The ozonation and HC hybrid system mostly follows the first order kinetics. Flow rate of O_3 above 2 gh^{-1} has marginal impact on degradation, however, again dependency relates to the COD content.

2.1. Pathways for the combined treatment process of HC /Ozone

Degradation of pollutants through direct reaction pathway involves the direct oxidation of the dissolved pollutant by O_3 at various pH or the indirect pathway by reaction with generated •OH through the decomposition of O_3 in water (Fig. 1). In respect to HC-based processes, at low temperature and atmospheric pressure, free radicals are generated by cavitational effects (i.e., sonolysis). These as-generated energized radicals can initiate a sequence of chain reactions with O_3 and water, forming additional free radicals. Secondly, O_3 can be directly converted to •OH during the collapse of cavitation bubbles. Radicals formed in aqueous media initiate successive chain reactions, which represents a combination of radical species used for the removal of recalcitrant pollutants. In fact, the synergistic effect in HC/O_3 eliminates the disadvantages of individual processes, substantially enhancing the degradation performance. Distinctly, HC/O_3 showed effective degradation of 2,4,6-trichlorophenol, potassium thiocyanate and 2,2-dichlorovinyl dimethyl phosphate within 120 min resulting in ξ of 1.48, 1.55 and 2.10, respectively. The concentration of the treated contaminants was > 100 mgL^{-1} and the ozone dose in the range of 0.2–0.5 gh^{-1} was sufficient. In the case of real wastewaters, to achieve ξ of 1.13, 1.20, 1.42 with COD over 10 000 mgL^{-1}, the ozone dose in the range of 3–9.4 gh^{-1} was supplied. Comparable ozone dose of 2 gh^{-1} applied to a model solution containing 10 mgL^{-1} of naproxen resulted in ξ of 12.3, indicating further optimization of ozone supply.

Fig. 2 presents a conceptual diagram of possible mechanisms of pollutant degradation by HC/O_3. In the absence of HC, the mass transfer of O_3 in water and the corresponding reaction with pollutants follow pathway 1. Pathway 4 takes place in sole use of HC through pollutant pyrolysis inside the cavitation bubbles or through the reaction with •OH generated by sonolysis. Pathways 1, 2, and 4 follow the combination reaction of both HC and ozonation with the reaction rates different from the individual systems. Decomposition of O_3 by cavitation generates excess amount of •OH to react with pollutants (pathway 2) and subsequent generation of O_2 in pathways 2 and 4 decreases the degradation rate. In addition, O_3 can scavenge •OH *via* pathway 5 (•OH + $O_3 \rightarrow HO_2^{\cdot} + O_2$), by reducing both •OH and O_3 concentrations in aqueous phase. This may be useful or detrimental depending on the reactivity of O_3 with pollutants and selectivity of pathway 2 or 5. Enhanced mass transfer of O_3 by HC can lead to the transfer of extra O_3 from gas phase into the solution. In such scenario, •OH are scavenged and the O_3 decomposition is eventually inhibited [40]. At high concentrations, O_3 can quench the formation of cavitation because of high degree of bubble coalescence. For many cases, this may be the reason why negative synergies between HC and O_3 have been reported [18]. Reaction of O_3 with H_2O_2, which is generated by HC from •OH as well as H_2O_2 at bubbles interface, is another feasible pathway to increase the efficiency of the combined process. A simultaneous presence of O_3 and H_2O_2 in the solution can result in several reactions named as peroxone chemistry. It includes the enhanced formation of •OH as well as peroxide species, trioxidane (H_2O_3), and highly reactive singlet oxygen. It should be noted that the degradation pathway is significantly affected by operating conditions, i.e., pressure at the inlet, resulting cavitation number, temperature, pH, and O_3 concentration, managing all physical and chemical phenomena in the HC based treatment process.

3. Synergistic effect of HC and H_2O_2

Conventionally used in bleaching and organic synthesis, hydrogen peroxide (H_2O_2) has found an extensive application in the treatment and disinfection of municipal wastewater and industrial effluents. Nevertheless, H_2O_2 is commonly used for the preparation of organic peroxides, oxidation of phenol and delignification of wood. Along with a relatively high oxidation potential (1.78 V), application of H_2O_2 has several technological advantages, such as high solubility in water, broad range of operating temperature, simplicity in hardware design, environmentally friendliness·H_2O_2 is sufficient towards the degradation of chlorinated alkanes, carboxylic acids and polycyclic aromatic hydrocarbons [42]. In this case, the mechanism involves the reaction of organic pollutants with perhydroxyl anions, which are responsible for oxidation capability of H_2O_2. The perhydroxyl anions are formed through the decomposition of H_2O_2 as described in Eq. (2). The decomposition rate of H_2O_2 increases at acidic condition, while in basic media H_2O_2 is relatively stable. However, at basic pH, perhydroxyl radicals can be also formed due to the reaction between H_2O_2 and HO^- (Eq. (3)) [14,25,43].

$$H_2O_2 \leftrightarrow HO_2^- + H^+ \quad (2)$$

$$H_2O_2 + HO^- \rightarrow HO_2^- + H_2O \quad (3)$$

The initial step of the reaction between HO_2^- and organic compounds involves the formation of the adduct that undergo further internal rearrangements [25]. Subsequently, the adduct is converted to the intermediate *via* the mechanism, which includes anion elimination or the migration of an alkyl radical with free electron pair. Resulting oxygen containing intermediates has higher stability than the parent compound, so the further degradation proceeds slowly. The effective degradation of organic pollutants *via* direct oxidation using H_2O_2 as a sole oxidant is possible in the systems with lower concentration of primary pollutants. In terms of wastewater treatment, to achieve noticeable COD reduction, it requires larger dosage of H_2O_2 and longer treatment time. Hence, the alternative mechanism based on the activation of H_2O_2 producing highly reactive HO• radicals is much more effective. The methods based on such mechanism fully unleash the oxidation potential of H_2O_2 and considered as AOPs. For instance, the photolytic excitation of H_2O_2 by UV ([H_2O_2] = 700 ppm, C_o = 630 ppm, pH 10) accel-

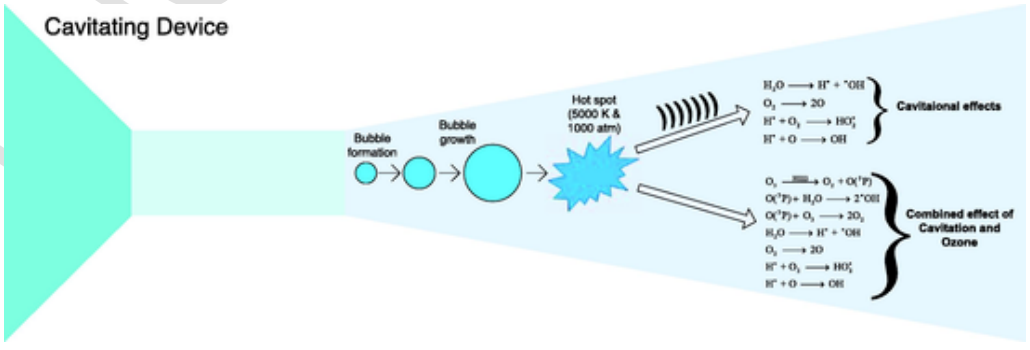

Fig. 1. Reactions involved in HC/O_3 process.

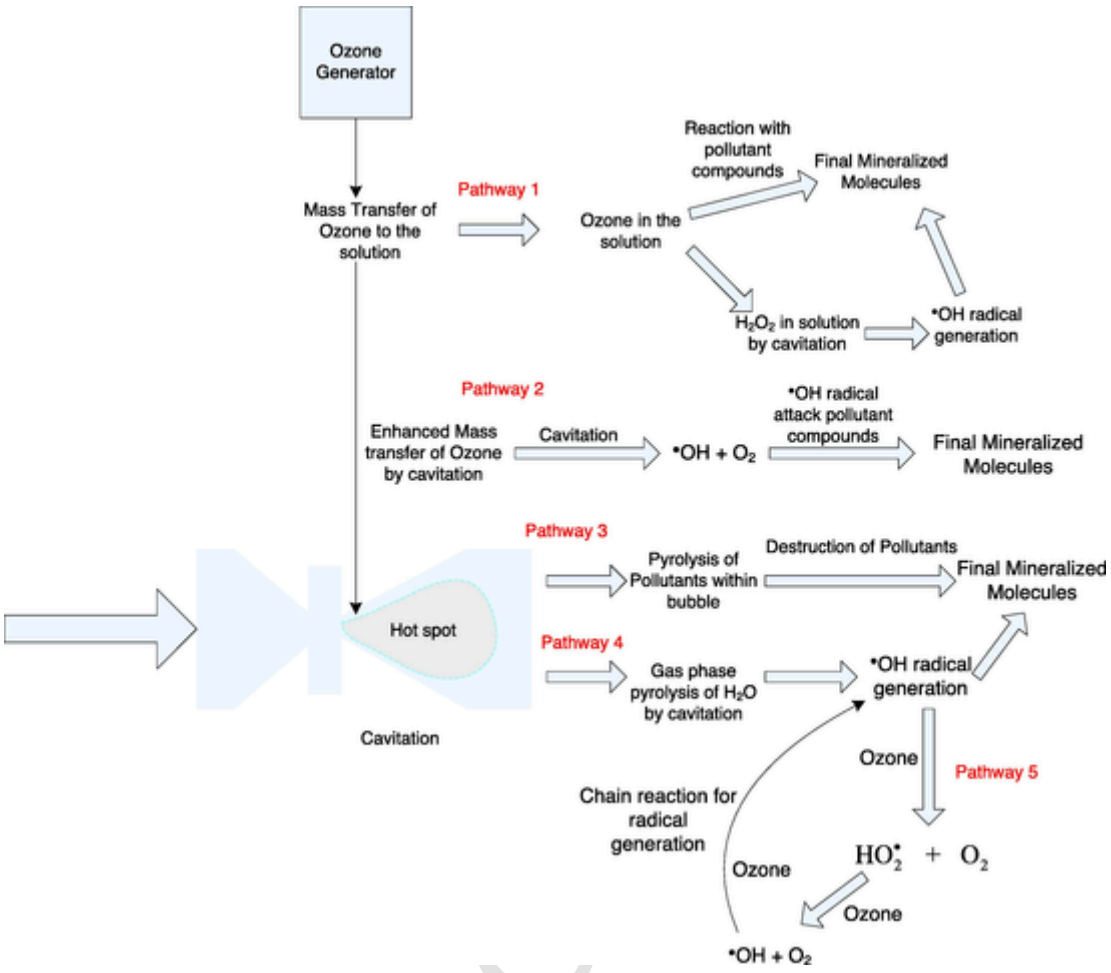

Fig. 2. Conceptual pathways for the degradation of pollutants in HC/O_3 . adapted from [41]

erated the degradation rate of 4-chloro-2-nitrophenol from 0.34×10^{-3} min^{-1} to 0.72×10^{-3} min^{-1} compared to the sole application of H_2O_2 [44]. Likewise, H_2O_2 in the presence of urchinlike manganese dioxide/biochar nanocomposites (α-MnO_2/BCs) completely degraded bisphenol A , under the ultrasound within 20 min ([H_2O_2] = 10 mM, C_o = 100 μM, [α-MnO_2/BCs] = 0.5 gL^{-1}, US 20 kHz, pH 7) and the kinetics were increased from 0.0002 min^{-1} to 0.0465 min^{-1} [45]. In both studies, the enhanced degradation efficiency of H_2O_2-based AOPs towards contaminants was accounted to the generation of HO• radicals due to H_2O_2 decomposition.

In case of cavitation phenomenon, collapse of microbubbles characterized with extreme conditions of pressure and temperature causes the emission of a large magnitude of energy to the system. The emitted energy along with the extreme conditions inside the cavitating bubble are sufficient to convert H_2O_2 into HO• radicals. Recently reported studies on advances of water remediation using combined process of HC and H_2O_2 are presented in Table 2.

3.1. Limitations of HC and H_2O_2 process

Formation of ROS from H_2O_2 under HC can proceed through the direct cleavage of peroxide bond to yield HO• radicals as shown in Eq. (4) [25]. The mechanism can work even under highly alkaline conditions in both acoustic and hydrodynamic cavitation. The treatment of the industrial effluent from bitumen production by AC/H_2O_2 yielded 40% COD reduction after 360 min resulting in ξ of 1.79 [17]. Apart from radical oxidation, the contaminants can be decomposed *via* direct pyrolysis inside the bubble interior.

$$H_2O_2 + cavitation \rightarrow HO^{\cdot} + HO^{\cdot} \quad (4)$$

The predominant role of HO• radicals in degradation of pollutants in HC/H_2O_2 was confirmed by Zupanc et al. [56] HC combined with 2 gL^{-1} H_2O_2 increased the TOC reduction of industrial pesticide effluent by 16.27% in 120 min. However, TOC removal rate was increased marginally from 3.86×10^{-3} min^{-1} to 6.02×10^{-3} min^{-1} when the H_2O_2 loading was increased to 5 gL^{-1} and 10 gL^{-1}, respectively [35]. High loadings of H_2O_2 have a scavenging effect on HC/H_2O_2 due to the formation of low reactive radicals forming through radical recombination reactions and the reaction of radicals with H_2O_2 (Eqs. 5–9) [25,49,50]. Therefore, the determination of the optimal loading of H_2O_2 is required as beyond a certain level of concentration of H_2O_2 the effect of scavenging reactions becomes considerable [57]. Additionally, the presence of H_2O_2 in high concentrations can cause the generation of vaporous cavities thereby lowering the cavitation intensity [58].

$$HO^{\cdot} + HO^{\cdot} + cavitation \rightarrow H_2O_2 \quad (5)$$
$$HO_2^{\cdot} + HO_2^{\cdot} + cavitation \rightarrow H_2O_2 + O_2 \quad (6)$$
$$HO^{\cdot} + HO_2^{\cdot} \rightarrow H_2O + O_2 \quad (7)$$
$$HO^{\cdot} + H_2O_2 + cavitation \rightarrow H_2O + HO_2^{\cdot} \quad (8)$$
$$HO^{\cdot} + O_2 + cavitation \rightarrow HO_2^{\cdot} + O^{\cdot} \quad (9)$$

Rajoriya et al. performed the degradation of reactive blue 13 dye using HC/H_2O_2 at an optimized inlet pressure of 4 bar in slit venturi and pH 2 [48]. They varied the molar ratio of dye to H_2O_2 concentration in the range of 1:1 to 1:40. The maximum decolorization rate of 46.6×10^{-3} min^{-1} with ξ of 3.47 was observed at the molar ratio of

Table 2
Application of HC/H_2O_2 process for the treatment of various pollutants and effluents.

Treated compound/wastewater	Conc. (mgL^{-1})	ξ	Process conditions	k (min^{-1})	Efficiency/contact time, (%/min)	Ref.
Bitumen production effluent	20000–22000	1.79	US 25 kHz 1000 W [H_2O_2] 71.92 gL^{-1} pH 10.5	–	COD 40/360	[17]
2,4,6-trichlorophenol	20	1.8	Inlet pressure: 4 bar [H_2O_2] 0.02 gL^{-1} pH 7	8×10^{-3}	62/120	[31]
Coomassie brilliant blue	20	2.11	Inlet pressure: 7 bar [H_2O_2] 0.67 gL^{-1}	27	TOC~66/60	[46]
Real industrial effluent	14.400	2.75	Inlet pressure: 4 bar[H_2O_2] 5 gL^{-1} pH 4	4.4×10^{-3}	COD40/120	[47]
Reactive blue 13	30	3.47	Inlet pressure: 4 bar [H_2O_2] 0.02 gL^{-1} pH 2	46.6×10^{-3}	91/120	[48]
Reactive orange 4	40	3.87	Inlet pressure: 5 bar [H_2O_2] 0.05 gL^{-1}pH 2	5.16×10^{-3}	TOC~32/60	[49]
Rhodamine 6G	10	4.24	Inlet pressure: 5 bar[H_2O_2] 0.02 gL^{-1}pH 10	21.6×10^{-3}	~54/120	[34]
Sodium dodecyl sulphate	10	4.81	Inlet pressure: 5 bar[H_2O_2] 5 gL^{-1}pH 2	71.2×10^{-3}	98/60	[50]
Methomyl	25	5.8	Inlet pressure: 5 bar[H_2O_2] 0.16 gL^{-1}pH 2.5	22.23×10^{-3}	97/60	[51]
Imidacloprid	20	11.15	Inlet pressure: 4 bar[H_2O_2] 0.08 gL^{-1}pH 3	41.37×10^{-3}	99/120	[52]
Methylene blue dye	50	11.79	Inlet pressure: 5 bar[H_2O_2] 0.1 gL^{-1}pH 2	91.68×10^{-3}	95/60	[53]
Imidacloprid	25	22.79	Inlet pressure: 15 bar[H_2O_2] 0.2 gL^{-1}pH 2.7	122.216×10^{-3}	100/45	[54]
Ternary dye wastewater	30	28.97	Inlet pressure: 6 bar[H_2O_2] 1:40pH 3	149.53×10^{-3}	100/40	[55]

1:20, while higher dosages of H_2O_2 were detrimental. Similarly, the study of different concentration proportions of H_2O_2 to 2,4,6-trichlorophenol (from 1:1 to 1:7) under HC showed that the degradation rate reached 8×10^{-3} min^{-1} at 1:5 within 120 min and was decreased to 6.3×10^{-3} min^{-1} at 1:7 [31]. Mukherjee et al. compared the effect of various H_2O_2 concentration (1 gL^{-1}, 5 gL^{-1} and 7 gL^{-1}) on sodium dodecyl sulfate under HC [50]. The maximum degradation degree of 98.37% with a rate constant of 71.2×10^{-3} and ξ of 4.81 was obtained using 5 gL^{-1} H_2O_2 in 60 min at pH 2. Increase of pH to 10 resulted in significant reduction of the degradation efficiency of HC/H_2O_2. The enhanced performance of HC/H_2O_2 at acidic conditions was confirmed by other studies. It was stated that dyes remain in molecular state at acidic pH and migrate to the interfacial "gas–liquid" zone or into collapsing microbubbles due to their hydrophobicity. The molecules which are exposed to the regions with high concentration of radical species will undergo direct attack. Wang et al. showed that the acidic pH promotes the degradation of reactive brilliant red K-2BP in swirling jet-induced cavitation/H_2O_2 system [59]. The degradation efficiency of reactive brilliant red K-2BP was 97.2 % after 120 min at pH 2, whereas it reached only 48.4 % at pH 10. It was also postulated that the enhancing effect was contributed by the increased oxidation potentials of HO• radicals and H_2O_2 in acidic medium. On the other hand, the study of rhodamine 6G degradation under HC/H_2O_2 varying the operating pH from 2 to 10 indicated the optimal pH at 10 [34]. It was proposed that due to pKa value of 6.13, rhodamine 6G exists in molecular state and exhibits hydrophobic properties as the free electron pair on the amine nitrogen donate charges to aromatic rings. As a result, rhodamine 6G easily diffuse to the "gas–liquid" region with high concentration of HO• radicals and undergo degradation. High ξ values (i.e., 11.15, 11.79, 22.78, 28.97) obtained for the degradation of imidacloprid and dyes indicate a strong oxidative capability of HC/H_2O_2 process. However, the concentration of pollutants can presumably be decreased due to the transformation into other recalcitrant states. In this case, it is important to use TOC or COD removal profiles to confirm the obtained results. Optimization of pH considering pKa of the treated contaminant along with prevention of scavenging/radical recombination reactions using optimal dose of H_2O_2 or employing stepwise feeding mode can be recommended for HC/H_2O_2. Major highlights of the reported work shows that the higher addition of H_2O_2 will have detrimental effect onto the degradation. Most of HC alongside H_2O_2 follows the first order kinetics. The presence of surfactant for e.g., Sodium dodecyl sulphate forms a favorable condition, allowing the components to reach the cavitation zone, hence the degradation will be higher. It was also found, that in case of HC and H2O2 based treatment process, long chain compounds are easily degraded comparing to the cyclic compounds.

4. Synergistic effect of HC and Fenton's process

Fenton's process mechanism has been reported by various researchers [60,61]. Fenton's process uses peroxide (generally H_2O_2) with iron ions to generate active oxygen species that degrade organic or even inorganic compounds [62]. The first Fenton reaction was found by H.J.H. Fenton in 1894, who reported that ferrous (Fe^{2+}) salts could activate H_2O_2 to degrade tartaric acid [63]. It has many advantages, including enhanced efficiency and non-toxicity for oxidation of organic compounds·H_2O_2 can be converted into reactive •OH that oxidizes organic pollutants to CO_2, H_2O [64-66]. The traditional Fenton's process involves ferrous oxidation to ferric ions and decomposition of H_2O_2 into •OH, as represented by Eq. (10).

$$Fe^{2+} + H_2O_2 \rightarrow Fe^{3+} + HO^- + HO^{\cdot} \quad (10)$$

The major drawbacks of the process are the radical scavenging impact of H_2O_2 and its self-decomposition. Moreover, when pH is above 3, the accumulated Fe^{3+} ions precipitate in the form of inactive amorphous ferric oxyhydroxides ($Fe_2O_3{\cdot}nH_2O$) [67]. As a result, individual AOP's processes are not yet named as commercially feasible. Hence, combining different of AOPs is considered as an essential step in to enhance the efficacy of processes. In recent years, a number of researches intensified the rate of degradation or attained full mineralization by combining HC with Fenton chemistry [68,69]. The HC/Fenton process with 0.05 gL^{-1} of Fe^{2+} degraded 91% of Reactive Brilliant Red K-2BP within 60 min, resulting in ξ 2.16. A ξ of 3.22 was obtained for congo red dye degradation using 0.025 gL^{-1} and inlet pressure of 4 bar within 120 min, while the utilization of 1 gL^{-1} Fe^{+2} and inlet pressure of 15 bar degraded 25 mgL^{-1} imidacloprid with ξ of 3.64 after 15 min of treatment. Employment of 0.18 gL^{-1} Fe^0 at inlet pressure 4 bar attained complete degradation of 20 mgL^{-1} imidacloprid in 60 min resulting in ξ of 5.7. These results suggest a strong correlation between ξ and process parameters and confirm that HC/Fenton process achieves high degradation effectiveness, because of the enhanced formation of quantum-free radicals [64,70]. Table 3 highlights the various illustrative researches on the synergistic effect between the HC and Fenton's reaction for wastewater treatment.

From the reports it is important to conclude that the Fenton with hydrodynamic cavitation process shows better synergistic effects in case of the cyclic compound's degradation. Pressure above 3 bars is sufficient to obtain cavitation conditions in used configurations of the treatment systems. The effluent pH, mostly acidic pH reveals an optimum condition. However, the neutralization of higher pH effluents to obtain preferred acidic conditions, is again one of the major limitations of the HC/Fenton based hybrid process. In real case scenario there is a chance

Table 3
Fenton technology for treating various organic pollutants and industrial effluents.

Treated compound/wastewater	Conc. (mgL^{-1})	ξ	Process conditions	k (min^{-1})	Efficiency/contact time, (%/min)	Ref.
p-nitrophenol	5000	–	Inlet pressure 3 bar[Fe^0] 1 gL^{-1}[H_2O_2] 7.5 gL^{-1}pH 3.8	–	63.2/90	[69]
Dichlorvos	20	–	Inlet pressure 5 bar[Fe^0] 3 gL^{-1}[H_2O_2] 1 gL^{-1}pH 3	40 × 10^{-3}	91.5/60	[71]
Methyl parathion	20	–	Inlet pressure 4 bar[Fe^{2+}] 1.5 gL^{-1}[H_2O_2] 0.1 gL^{-1}pH 3	6.36 × 10^{--3}	93.8/120	[72]
Orange G	20	1.56	Inlet pressure 3 bar[Fe^0] 0.7 gL^{-1}[H_2O_2] 0.02 gL^{-1}pH 3	8.26 × 10^{-3}	99.8/20	[73]
Tannery effluent	9760	1.73	Inlet pressure 5 bar[Fe^0] 3 gL^{-1}[H_2O_2] 9.51 gL^{-1}pH ~ 7	0.71 × 10^{-3}	COD 50.2/120	[27]
Reactive brilliant red K-2BP	10	2.16	Inlet pressure 4 bar[Fe^{2+}] 0.05 gL^{-1}[H_2O_2] 0.1 gL^{-1}pH 4	40.3 × 10^{-3}	91/60	[74]
Industrial wastewater	~100000	2.67	Inlet pressure 4 bar[Fe^0] 1 gL^{-1}[H_2O_2] 20 gL^{-1}pH 13.2	3.2 × 10^{-3}	COD42/170	[75]
Methyl orange	5	3.13	Inlet pressure 4 bar[Fe^0] 0.02 gL^{-1}[H_2O_2] 0.33 gL^{-1}pH 2	9.4 × 10^{-3}	90.15/60	[76]
Congo red	20	3.22	Inlet pressure 4 bar[Fe^{2+}] 0.025 gL^{-1}[H_2O_2] 1.0 gL^{--1}pH 3	15.3 × 10^{-3}	70/60	[77]
Imidacloprid	25	3.64	Inlet pressure 15 bar[Fe^{2+}] 1 gL^{-1}[H_2O_2] 5.2 gL^{-1}pH 2.7	250.74 × 10^{-3}	97.77/15	[78]
Imidacloprid	20	5.7	Inlet pressure 4 bar[Fe^0] 0.178 gL^{-1}[H_2O_2] 0.08 gL^{-1}pH 3	162.25 × 10^{-3}	100/60	[52]
Ternary dye	30	6.28	Inlet pressure 6 bar[Fe^{2+}] 1 gL^{-1}[H_2O_2] 30 gL^{-1}pH 3	203.14 × 10^{-3}	98.28/20	[55]
2,4-dinitrophenol	20	12.5	Inlet pressure 4 bar[Fe^{2+}] 0.3 gL^{-1}[H_2O_2] 0.1 gL^{-1}pH 4	16.5 × 10^{-3}	83.42/120	[79]

to mix few different effluent streams to "blend" an optimal composition of treated wastewater.

4.1. Limitations of HC and Fenton's process

Homogeneous Fenton's reaction *via* iron ions (Fe^{2+} or Fe^{3+}) offers better process effectiveness because mass transfer restriction of active species is negligible. Although Fe^{2+} is dissolved even at neutral pH conditions, Fe^{3+} vanishes at pH value of 4, forming ferric hydroxide sludge. For practical applications, rigorous acidic pH conditions (pH < 4) are needed, which requires chemicals to neutralize effluent before discharge [80,81]. Production and subsequent disposal of iron hydroxide sludge remain a major drawback for the application of conventional Fenton's process, although these hydroxide complexes can be recycled by UV or solar light irradiation. These reuse procedures require strict maintenance of pH, which is highly costly. In addition, the necessary Fe^{2+} concentration range for individual treatment processes is 50–80 ppm [82], which is obviously above the minimum limit enforced by the Directives of the European Union (EU) for direct release of sewage into the environment [83]. Fenton-based AOPs demonstrate serious practical disadvantages; therefore, studies are concentrated on finding new Fenton catalysts to produce •OH from H_2O_2 that are practically acceptable and economically viable.

Wu et al. utilized zerovalent aluminum as the Fenton-type catalyst to generate •OH for oxidative removal of arsenite [84]. The decomposition of H_2O_2 into •OH by this method has many benefits e.g., natural availability and lightweight. This prompted researchers to look for alternative compounds similar to the Fenton process Cerium (Ce) is proposed as the only metal of lanthanide group activating H_2O_2 through Fenton-like mechanism. It is the only rare earth element exhibiting both + 3 and + 4 oxidation states owing to its $4f_2$ $6 s_2$ valence formation. Chen et al. demonstrated that the response between Ce^{3+} and H_2O_2 results in the generation of reactive species (Ce^{3+}–OOH^-) *via* surface alteration in the presence of sulfate groups. Sulfate groups act as acidic sites to decompose the peroxide species into •OH through acid catalyzed intramolecular transfer of electrons, and to promote the redox conversion of Ce^{3+} to Ce^{4+} [85].

H_2O_2 as both oxidizing and reducing agent, plays an essential role in the oxidation of Cr(III) to Cr(VI), resulting in the regeneration of Cr(VI) reduction. Each redox conversion [Cr(III) to Cr(VI) and Cr(VI) to Cr (III)] is accompanied by the generation of •OH without sludge formation. All these reactions can be easily attained by controlling the pH. Bokare and Choi demonstrated that the pH-mediated redox cycle Cr(III) to Cr(VI) promoted •OH generation under both alkaline and neutral mediums for the degradation of 4-chlorophenol [86]. Divalent cobalt ion (Co^{2+}) has been widely examined as a Fenton-like catalyst to generate •OH using the Co^{2+}/Co^{3+} redox pair [$E_0(Co^{3+}/Co^{2+}) = +1.92$ V] [87-89].

The commonly accepted free radical chain mechanism of Fenton's process is presented in Fig. 3. Fenton's free radical mechanism has been challenged from time to time, and many researchers confirmed the involvement of reactive species other than •OH. The constraints in the solubility of iron species prompted researchers to focus on iron free Fenton like systems, where generation of •OH follows the similar path-

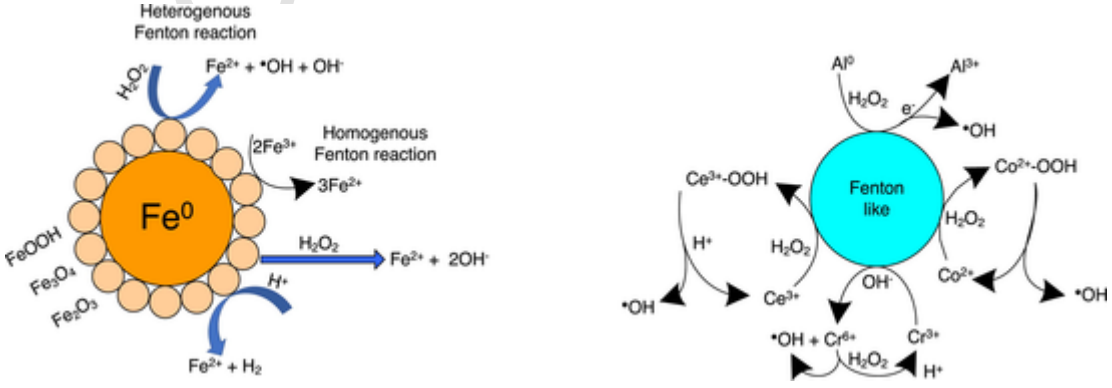

Fig. 3. Pathways of •OH production in Fenton's and Fenton-like oxidation [86].

way as Fenton's oxidation (Fig. 3). Catalytic materials with various oxidation states and redox stability effectively decompose H_2O_2 to produce •OH under both homogeneous, heterogeneous response, or even neutral/alkaline conditions. Each non-ferrous catalyst has demerits, which can offset the practical benefits of greater catalyst stability and neutral pH range.

The effectiveness of the cavitation/Fenton process can be significantly improved by UV assistance. UV irradiation in cavitation-photo-Fenton maximizes the efficiency of •OH generation reducing the loss of •OH [90]. Dükkanci et al. applied the hybrid technique of US/photo-Fenton to the oxidation of bisphenol A (BPA) [91]. From the results, it was found that US plays an important role in BPA decomposition because of the sonoluminescence and pyrolysis caused by sonocavitation. Application of sonocavitation improved antipyrine TOC removal of photo-Fenton process from 75% to 79% within 50 min and increased the rate constant from 0.0398 min^{-1} to 0.0466 min^{-1} [92]. Many researchers have reported that hybrid Fenton processes (e.g., sonocavitation electro-Fenton, and solar sonocavitation electro Fenton) can achieve considerably higher efficiency in water remediation [93-95].

5. Synergistic effect of HC and peroxydisulphate (PDS) process

Sulfate anion radicals ($SO_4^{\bullet-}$) has received great attention as an alternative to •OH. $SO_4^{\bullet-}$ has high oxidation potential (2.5–3.1 V) and is non-selective for degradation of organic pollutants [96-100]. $SO_4^{\bullet-}$ reacts with pollutants and results in partial or complete mineralization. PDS and peroxymonosulfate (PMS) are strong environmental oxidants. The standard oxidation–reduction potential of PDS is equal to 2.01 V which is higher than that of PMS with the oxidation–reduction potential of 1.80 V (Eqs. (11), 12).

$$S_2O_8^{2-} + 2H^+ + 2e^- \rightarrow 2HSO_4^- \quad (11)$$

$$HSO_5^- + 2H^+ + 2e^- \rightarrow HSO_4^- + H_2O \quad (12)$$

Oxidation by activated PDS can be preferred over HO•-based methods as PDS is more stable and transported to the subsurface before being activated for the degradation of various contaminants. PDS produces $SO_4^{\bullet-}$ with a greater oxidative capability in certain circumstances (e.g., activation by heat, US, and UV) [101]. Under alkaline conditions, $SO_4^{\bullet-}$ transform into •OH. Furthermore, $SO_4^{\bullet-}$ can react with water to generate •OH [102,103]. PDS is chemically stable, has high reusable and recyclable nature. Studies regarding the combined processes of PDS and HC were summarized in Table 4.

Bagal and Gogate studied the degradation of 2,4-dinitrophenol by combining HC and PDS activated by ferrous ions [79]. The combined approach enhanced the degradation of 2.4-dinitrophenol resulting in ξ of 3.20. Choi et al. confirmed that the oxidation of BPA was enhanced by both •OH and $SO_4^{\bullet-}$ (ξ 2.23), reaction rate was increased from 1.0×10^{-3} min^{-1} to 12.7×10^{-3} min^{-1} [20]. Wang and Zhou showed that the activation of PDS induced by US at the acidic pH favored the complete oxidation of contaminants [105]. They also showed that the free radicals produced by PDS activated by acoustic cavitation have a higher oxidation potential. As a result, 89.4% of carbamazepine was removed at pH 5 and the PDS concentration of 5 $mmolL^{-1}$ within 120 min. Li et al. studied the degradation of trichloroethane (TCE) using various US frequency [108]. At higher US frequency, the activation of PDS was faster. At 400 kHz, the acoustic cavitation activated PDS removed 90% of the TCE in 60 min. Wang et al. concluded that acidic conditions (pH 3) and high temperature enhanced the activity of PDS [106]. Application of cavitational energy gave ξ of 2.02 by promoting the generation of $SO_4^{\bullet-}$, which increased TOC removal up to 90 % within 120 min. Deng et al. studied the degradation of phenanthrene by coupling sonocavitation with PDS [107]. As the soil slurry absorbed the cavitational energy, the resultant hot soil activated PDS inducing rapid oxidation of phenanthrene.

5.1. Pathways and limitations of HC/PDS

Formation of reactive radicals in PDS and PMS-based processes is accomplished through thermal, radiolytic, UV and cavitation activation. The efficacy of PDS-based treatment processes is affected by several variables such as the rate of $S_2O_8^{2-}$ activation, nature of the activating agent, and organic contaminant and oxygen concentrations in the environment [109,110]. The energy applied during activation causes the cleavage of peroxide bonds and yield of $SO_4^{-\bullet}$ as displayed in the following equations:

$$S_2O_8^{2-} + energy\ input \rightarrow 2SO_4^{\bullet-} \quad (13)$$

$$S_2O_8^{2-} + e^- \rightarrow SO_4^{2-} + SO_4^{\bullet-} \quad (14)$$

Dissociation of peroxide bonds in PDS can be done by US or HC. The synergistic effect of the combined process of HC/PDS is more complex compared with that of individual processes. The enhanced effect of PDS oxidation is due to the secondary radicals propagating through as generated $SO_4^{\bullet-}$. Although $SO_4^{\bullet-}$ are the main reactive species exclusively produced by PDS activation, •OH as a secondary oxidizing agent may co-exist at alkaline conditions. In such systems •OH are formed *via* the reaction of $SO_4^{\bullet-}$ with water and HO^- [111]:

$$SO_4^{\bullet-} + H_2O \rightarrow SO_4^{2-} + HO^{\bullet} + H^+ \quad (15)$$

$$SO_4^{\bullet-} + HO^- \rightarrow SO_4^{2-} + HO^{\bullet} \quad (16)$$

Both •OH and $SO_4^{\bullet-}$ participate in degradation reactions. Unlike •OH, $SO_4^{\bullet-}$ reacts primarily by single electron transfer (SET), which is followed by several different reactions like hydroxylation, double bond addition, electron rearrangement depending on nature of the treated compound [112]. Pollutants with electron donating groups can spontaneously react with $SO_4^{\bullet-}$ though SET route creating organic cation radicals. The formed cation radicals having one free radical readily undergo subsequent degradation reactions. The overall degradation rate of cont-

Table 4
Summary of literature on wastewater treatment using HC/US-activated PDS oxidation.

Treated compound/wastewater	Conc. (mgL^{-1})	ξ	Process conditions	k (min^{-1})	Efficiency/contact time, (%/min)	Ref.
1.4-dioxane	1	1.52	US 400 kHz 100 W[$Na_2S_2O_8$] 0.36 gL^{-1}pH 7	0.00645	~95/300	[104]
Carbamazepine	5910	1.92	US 40 kHz 50 W[$K_2S_2O_8$] 0.27 gL^{-1}pH 3	0.48×10^{-3}	43.8/120	[105]
Humic acid	30	2.02	US 40 kHz 200 W[$K_2S_2O_8$] 23.8 gL^{-1}pH 3	1.48×10^{-3}	TOC > 90/120	[106]
Bisphenol A	10,040	2.23	Inlet pressure 5 bar[$Na_2S_2O_8$] 1.67 gL^{-1}pH 6	12.7×10^{-3}	80/120	[20]
2,4-dinitrophenol	20	3.20	Inlet pressure 5 bar[$Na_2S_2O_8$] 0.16 gL^{-1}[Fe^{2+}] 0.08 gL^{-1}pH 4	0.79×10^{-3}	55.3/120	[79]
Phenanthrene	–	3.51	US 20 kHz 90 W[$K_2S_2O_8$] 50 gL^{-1}pH 5.4	2.68×10^{-3}	>90/30	[107]
1,1,1-trichloroethane	50	3.94	US 400 kHz 100 W[$K_2S_2O_8$] 0.22 gL^{-1}pH 7	39.6×10^{-3}	100/120	[108]
1,1,1-trichloroethane	20	4.43	US 400 kHz 100 W[$Na_2S_2O_8$] 0.36 gL^{-1}pH 7	0.03365	100/240	[104]

aminants depends on the complex combination of $SO_4^{\bullet-}$ chain propagation.

$S_2O_8^{2-}$ can react directly with organic compounds without activation, but the elimination degree is poor due to lower oxidation potential. High pressure and temperature induced by cavitation lead to the homolysis of PDS as illustrated in Fig. 4. The homolytic disassociation of PDS proceeds in a similar energy-inducing mechanism as heat and UV activation [113,114].

The mechanism of HC/PDS combined process is seen as the synergistic effect between heat breakdown and free radical reactions. $SO_4^{\bullet-}$ is not sufficiently produced *via* PDS activation at the initial stage. Therefore, the dominant mechanism for decomposition of organic compounds is the pyrolytic degradation within the bubble or near interphase. This is possible due to elevated temperature and pressure inside the cavitating bubble, which occurs at a short timescale. In addition, water vapor undergoes heat disassociation to yield reactive $^{\bullet}OH$ and hydrogen atoms. Owing to its activation effect on PDS, the amount of $SO_4^{\bullet-}$ can be dramatically increased over time and the sequence of reactions produce specific reactive radicals. Hence, both $SO_4^{\bullet-}$ and $^{\bullet}OH$ are considered as the dominant species responsible for the degradation of contaminants by HC-based processes. However, due to complex molecular structure and functional groups of organic pollutants and radical reactions the oxidation mechanism in HC/PDS is still under discussion. To unfold degradation pathways, the identification of intermediates is required. There are many influential factors in the degradation of cavitation-activated PDS, such as pH, PDS concentration, input power, frequency of sonocavitation equipment, and co-existing inorganic ions. Hao et al. studied different power intensities (i.e., 3.49, 6.98, 10.47, 3.96, and 17.44 Wcm^{-2}) for the degradation of ammonium perfluorooctanoate, and found that a power intensity of 10.47 Wcm^{-2} led to the highest defluorination ratio [113]. Chen and Huang found that TOC removal rate of dinitrotoluene increased with the increase of power intensity, while the higher power intensity of 222 Wcm^{-2} was detrimental to TOC reduction [115]. Regarding the pH effect on US/PDS system, Wei et al. found that production of radicals was highest at basic pH [116]. The lower radical production by US-activated PDS were observed at pH 3.5 and 7.4, while US accelerated the base activation of PDS at pH 9.4. On contrary, Chen and Su postulated that the degradation of dinitrotoluenes was increased by decreasing the solution pH up to 0.2 [117]. It was proposed that the production rate of $SO_4^{\bullet-}$ increases under acidic conditions:

$$S_2O_8^{2-} + H^+ \rightarrow HS_2O_8^- \quad (17)$$

$$HS_2O_8^- \rightarrow SO_4^{\bullet-} + SO_4^{2-} + H^+ \quad (18)$$

In strong acidic conditions (pH < 1), PDS exists in its protonated form (pKa ~ 1), which is known to undergo heterolytic dissociation resulting in formation of HSO_4^-, H_2SO_5, H_2O_2 [116,118]. Since H_2SO_5, H_2O_2 are weak oxidants, it is reasonable to clarify the contribution of their activation under the conditions of acoustic cavitation.

6. Synergistic effect of HC and photocatalytic oxidation

Combination of HC with catalysts was proved energy efficient towards a variety of chemical processes, such as organic synthesis, hydrolysis of oils, depolymerization, transesterification and cracking of petroleum crude [119]. It was proposed that in such systems the mechanical effect of cavitation intensifies the reaction and the catalyst with high surface area and porosity gets activated by asymmetric cavity collapse on its surface. Photocatalytic process initiated on the surface of semiconductors (TiO_2, ZnO, Nb_2O_5) under UV or solar irradiation was also combined with HC and widely applied for the degradation of pollutants [55,78,120]. The activation of semiconductors results in the formation of electron/hole pair, which initiate the dissociation of water by electron transfer mechanism to yield $HO^{\bullet}$ radicals. Compared to homogeneous catalysis (i.e., HC/Fenton), the use of solid catalysts in HC precludes the formation of sludge which requires additional stage of treatment [11]. Moreover, the catalyst may undergo regeneration throughout the process, thereby lowering the cost of treatment. As observed by Wang et al. HC also prevents the agglomeration of catalyst particles and provides better contact between the catalyst surface and the contaminant treated [121]. This was possible due to the constant refresh of TiO_2 surface by the effect of shear stress and micro-streaming induced by cavitation. As a result, when water jet cavitation was combined with TiO_2, the degradation of reactive red 120 was elevated by 136 % in 90 min compared to the individual processes. In this study, TiO_2 particles were dispersed in the reaction mixture placed inside the jacketed glass reactor equipped with a source of jet cavitation and 9 W mercury lamp. Bagal and Gogate investigated the degradation of diclofenac sodium in TiO_2/UV system combined with HC using slit venturi as a cavitating device [122]. Under the selected optimal conditions, the presence of 0.2 g/L TiO_2 enhanced the degradation efficiency of HC/UV from 65.53 % to 79.38 % within 120 min. The addition of 0.2 g/L H_2O_2 in HC/TiO_2/UV system further improved the degradation rate of diclofenac sodium from 0.0143 min^{-1} to 0.026 min^{-1} and increased ξ from 1.43 to 2.5. The role of H_2O_2 in HC/TiO_2/UV was assigned to the generation of $HO^{\bullet}$ radicals and the inhibition of undesired recombination of electron/hole pairs. On the other hand, the oxidation of pollutants in the combined process of photocatalytic oxidation and HC can be conducted in the absence of UV. Thus, Li et al. studied the degradation of rhodamine b in HC in the presence of Fe^{3+}-doped TiO_2 [123]. The activation of Fe^{3+}-doped TiO_2 to generate electron/hole pair was achieved due to the cavitation luminescence in HC. It was found that doping with Fe^{3+} broadened the optical adsorption of TiO_2 enhancing the utilization of the light energy and activity. The addition 0.5 g/L Fe^{3+}-doped TiO_2 photocatalysts improved the degradation efficiency of rhodamine b under HC from 58.32 % to 91.11 % after 150 min of treatment. Parsa and Zonouizian tested scrap iron sheets as a catalyst in HC reactor for the degradation of rhodamine b and confirmed the importance of the catalyst exposure mode [124]. They compared submerged and inline location of the catalyst towards the cavitating device and ob-

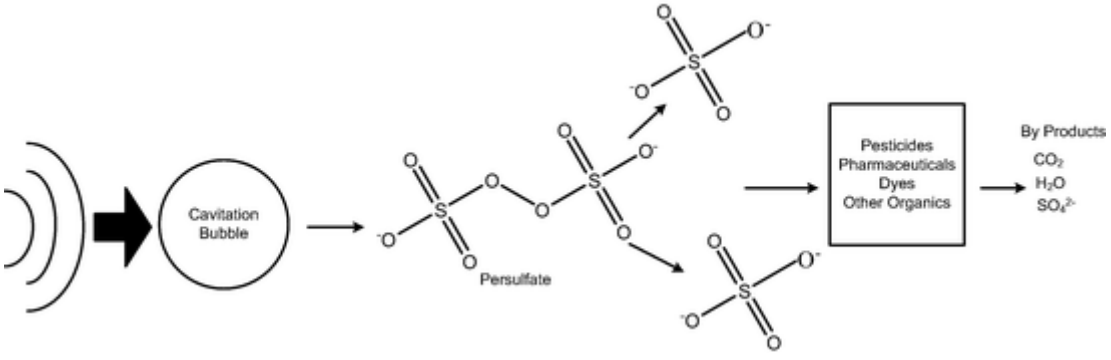

Fig. 4. PDS activation by HC.

tained 73 % and 39 % of rhodamine decolorization in 240 min, respectively. Higher decolorization extend in submerged operation mode was attributed to the lower distance between the catalyst and cavitating jets, where collapsing microbubbles impinge on the surface of the catalyst by providing more reactive sites. The overview of work done in the area of HC and photocatalytic oxidation is shown in Table 5.

6.1. Pathways and limitations of HC/Photocatalytic oxidation

Photocatalyst technology produces reactive radicals absorbing the energy of photons as a source of activation. In the view of water treatment, the photocatalytic oxidation process as an effective, environmentally friendly and economically feasible alternative to the existing water treatment technology has attracted great attention from the scientific community. Photocatalysis employs semiconductor oxides (e.g., TiO_2, ZnO, CuO) due to their intrinsic features such as smaller band gap energy, stability, ease of production and non-toxicity [128,129]. The principal mechanism of photocatalysis relies on the initial stage of activation, where the photocatalyst absorbs photon energy equal or greater than its band gap energy. This causes the excitation of an electron (e^-) in the valence band (VB) and subsequent migration to the conduction band (CB), leaving photogenerated holes (h^+) in the valence gap [128-130]. Electron/hole pairs can react with O_2 and water to yield reactive radicals and H_2O_2 as summarized in Eqs. 19–23·H_2O_2 is decomposed to HO• radicals under cavitation (Eq. (4)):

$$MeO + h\nu \rightarrow e^-_{CB}(MeO) + h^+_{VB}(MeO) \quad (19)$$

$$e^-_{CB}(MeO) + O_2 \rightarrow O_2^{\cdot} \quad (20)$$

$$O_2^{\cdot} + H_2O + H^+ \rightarrow H_2O_2 + O_2 \quad (21)$$

$$h^+_{VB}(MeO) + H_2O \rightarrow HO^{\cdot} + H^+ \quad (22)$$

$$2h^+_{VB}(MeO) + 2H_2O \rightarrow H_2O_2 + 2H^+ \quad (23)$$

The production of reactive species in hybrid HC/Photocatalytic oxidation process can be decreased due to the recombination of electron/hole pairs and photoexcited e^- can be captured by HO• radicals:

$$e^-_{CB}(MeO) + h^+_{VB}(MeO) \rightarrow MeO + heat \quad (24)$$

$$e^-_{CB}(MeO) + HO^{\cdot} \rightarrow HO^- \quad (25)$$

To reduce the recombination of electron/hole pairs, Behti et al. reported doped TiO_2 nanoparticles synthesis with transition metals (i.e., Fe and Ce) for degradation of crystal violet dye under HC and UV [126]. 94 % of crystal violet dye was degraded in 90 min in the presence of 0.6 gL^{-1} TiO_2 giving ξ 3.52. Doping of TiO_2 with 0.8 % of Fe and 1.6 % of Ce increased the synergy to 4.26 and 3.87, respectively. Further increase of Fe content in TiO_2 to 1.6 % decreases the rate constant of dye degradation from 0.0332 min^{-1} to 0.017 min^{-1} indicating the requirement in optimization of the dopant loading. When the cavitation device and the connected UV source are operated sequentially, in the absence of a suitable electron/hole acceptor or donor, the recombination of electron/hole pairs may be important. For instance, the application of 0.2 gL^{-1} Nb_2O_5 in a sequentially connected HC/UV system degraded only 55.18% of imidacloprid in 120 min, showing ξ of 0.92 [78]. It was concluded that the antagonistic effect in HC/UV/Nb_2O_5 was also contributed by higher loadings of the photocatalyst, which decreased the cavitational intensity hindering the growth of microbubbles. It is assumed that the effect of cavitation overcome the mass transfer resistance associated with photocatalyst in the system and the presence of solid particles provides additional nuclei for cavitation bubble growth. On the other hand, high loadings of photocatalyst prevents the effective UV irradiation as the light penetration is hindered and the interaction between photocatalyst and UV is reduced. Thus, the degradation of reactive red 2 in HC/UV/TiO_2 varying the photocatalyst loading in the range of 25–500 mgL^{-1} showed higher degradation extend in lower concentration of the catalyst [121]. Predominantly, the degradation of the dye was increased till the optimal TiO_2 loading of 100 mgL^{-1} and gradually decreased at 200 mgL^{-1} and 500 mgL^{-1}, decreasing the synergistic effect from 2.9 to 1.33. This confirms that the hybrid HC/photocatalytic oxidation process operates with a lower dose of catalyst, combined with multiple reusability and ease of manufacturing, and has great potential in large-scale practical applications.

7. Experimental variables affecting synergism of HC-based AOPs

7.1. Effect of pH

Degradation efficiency of cavitation based AOPs is dependent. Many studies reported that the decrease in pH increases the degradation efficiency as the production of •OH is favored. In HC/Fenton processes, pH affects the oxidation potential by directly influencing Fe^{2+} concentration and the amount of •OH generated *via* the Fenton's reagent. The acidic pH favoring Fenton's processes in the narrow range of 3–4 is well known [131]. Lower pH of 2.5 favors the generation of $(Fe(II)(H_2O))^{2+}$ hindering the reactivity of Fe^{2+} with H_2O_2. Thus, the generation of •OH is lowered followed by the decline in degradation efficiency. Additionally, when pH is lower than 2.5, the possibility of formation of different Fe^{3+} complexes and the decomposition of •OH or H_2O_2 occur. Fenton based processes are complicated and dependent on iron species present in the bulk solution. The subsequent neutralization and precipitation of $Fe(OH)_3$ reduce the efficacy of the treatment processes [80,132,133]. Iron complex species $[Fe(II)(H_2O)_6]^{2+}$ are formed at pH ~ 2.0, which reacts slowly with H_2O_2 and, therefore, produce less HO•. Additionally, in the presence of high concentration of H^+, H_2O_2 may accept a proton and form low reactive oxonium ion ($H_3O_2^+$) which makes the H_2O_2 stable and electrophilic (Eq. (26)) [134,135]:

$$H_2O_2 + H^+ \rightarrow H_3O_2^+ \quad (26)$$

Bremmer et al investigated the effect of initial pH on the HC/Fenton process for the degradation of 2,4-dichlorophenoxyacetic acid [136]. At

Table 5
Application of HC/Photocatalysis for the treatment of various pollutants and effluents.

Treated compound/ wastewater	Conc. (mgL^{-1})	ξ	Process conditions	k (min^{-1})	Efficiency/contact time, (%/min)	Ref.
Imidacloprid	25	0.92	Inlet pressure: 15 bar[Nb_2O_5] 0.2 gL^{-1}UV 250 WpH 2.7	6.837×10^{-3}	55.18/120	[78]
Ternary dye	30	1.43	Inlet pressure: 6 bar[TiO_2] 0.2 gL^{-1}UV lamp 250 WpH 3	14.35×10^{-3}	82.13/120	[55]
Methylene blue	50	1.46	Inlet pressure: 5 bar[Bi/TiO_2] 0.2 gL^{-1}pH 2	8.62×10^{-3}	64.58/120	[53]
Reactive red 180	100	1.48	Inlet pressure: 5 bar[ZnO] 1.0 gL^{-1}pH ~ 7	8.3×10^{-3}	TOC 61.6/180COD 77.9/180	[120]
Antibiotic wastewater	236	2.12	Nozzle inlet pressure: 120 bar[TiO_2] 1.67 mgL^{-1}[H_2O_2] 500 mgL^{-1}[$FeSO_4$] 10 mgL^{-1}[$CuSO_4$] 3.33 mgL^{-1}UV lamp 30 WpH 2.7	0.0272	COD 79.9/60	[125]
Diclofenac sodium	20	2.5	Inlet pressure: 4 bar[TiO_2] 0.2 gL^{-1}[H_2O_2] 0.2 gL^{-1}UV lamp 250 WpH 4	0.026	94.78/120	[122]
Rhodamine B	10	–	Inlet pressure: 3 bar[Fe(III)/TiO_2] 0.5 gL^{-1}pH 7	–	91.11/150	[123]
Crystal violet dye	50	3.52	Inlet pressure: 5 bar[TiO_2] 0.6 gL^{-1}UV 125 WpH 6.5	0.0275	94/90	[126]
Methyl orange	10	4.25	Inlet pressure: 4 bar[Cu^0] 0.04 gL^{-1}pH 3	–	83/20	[127]

pH 2.5, it has been observed that the combination of HC and Fenton process enhanced TOC removal by 10% in comparison with individual Fenton process at the same pH. This suggests that cavitation conditions spread the range of pH applicable to the Fenton's reaction. Many researchers have reported that acidic conditions promote HC/Fenton for the treatment of phenol [79], textile dye [137], and pharmaceutical wastewaters [52]. Similarly, the COD removal of synthetic wastewater has been examined over the pH range of 2–4.5. The maximum COD and color removal were reported at pH 3 [138].

Oxidation during ozonation is carried out by two paths: (1) O_3 can be rapidly decomposed in solution to produce •OH and other free radical species at basic pH, and (2) it can react directly with organic compounds as an electrophile agent under acidic conditions. At cavitation conditions, O_3 can be thermolytically decomposed, forming O_2 and atomic oxygen which reacts with water to produce •OH as a result of chain reaction. Similarly, the combined process of HC/O_3 favors the enhanced mass transfer of O_3 to the solution attributed to the physical effect of HC. Through the direct O_3 attack and the production of •OH as a result of the decomposition of O_3, organic pollutants are, therefore, effectively degraded. During the cavitation and O_3 hybrid cycle, the following reactions are predicted:

$$O_3 \rightarrow O_2 + O(3P) \quad (27)$$

$$O(3P) + H_2O + \rightarrow 2HO^{\cdot} \quad (28)$$

It has been reported that the decomposition of reactive orange 4 in HC/O_3 (Venturi tube, inlet pressure 5 bar, 3 gh^{-1}) attained 76.25% of TOC reduction within 60 min. Gore et al. showed that the degradation of reactive orange 4 was higher in the combined process at pH 2 due to higher availability of •OH by effective dissociation of O_3 under cavitation [49]. Similarly, Barik and Gogate investigated the degradation of 4-chloro-2-aminophenol using the hybrid process of HC/O_3 over a wide pH range of 4–8 [26]. They reported that the maximum degradation of 40.86 % with ξ of 1.01 was achieved at pH 6. During the ozonation, an increase of pH from 4 to 6 resulted in O_3 instability and generation of more free radicals. Similar results were reported by He et al. for the treatment of *p*-aminophenol by O_3 [139]. The degradation of *p*-aminophenol was increased to 88 % when the initial pH was increased from 7 to 9. At pH 12, an excess amount of OH^- marginally reduced the degradation efficiency to 84 % due to the recombination of •OH.

When PDS (peroxydisulphate) is combined with HC to decompose persistent pollutants, the initial pH value of the solution will also affect the treatment effect. Wang and Zhou investigated the degradation of carbamazepine by sonocavitation/PDS at wide pH range of 3–11 [105]. The highest degradation efficiency of 54% was achieved at pH 5 due to the enhanced oxidation potential of •OH and the presence of $SO_4^{\bullet-}$. Despite the fact, some researchers observed PDS activation in basic conditions (pH 10.5) at 40 °C, where the ratio of PDS to the contaminant (r_{ox}) was 0.41. In such conditions HC/PDS gave better results removing 43% COD from the volatile organic compounds (VOCs) [140]. However, the results published by Darsinou et al. who investigated the degradation of BPA by sonocavitation-activated PDS showed deviations from the positive synergy [141]. They compared the degradation effectiveness over a large pH range (3–9). In pH range of 3–6, complete degradation of BPA was observed, whereas increase of pH to 9 resulted in adverse effect. When pH was increased, the degradation efficiency was reduced to 40% as PDS acquired higher stability at alkaline conditions. Compared with alkaline conditions, the diffusion of PDS is faster at acidic conditions as mentioned above in Eq. (17).

Number of studies reported that PDS can react with OH^- forming •OH under alkaline conditions. For instance, Fan et al. demonstrated that the predominant of •OH radical-based degradation pathway at alkaline conditions [142]. The generation of •OH from the PDS in alkaline conditions can be explained by the following equations [143].

$$2S_2O_8^{2-} + 2H_2O \rightarrow SO_4^{\cdot-} + 3SO_4^{2-} + O_2^{\cdot-} + 4H^+ \quad (29)$$

$$SO_4^{\cdot-} + HO^- \rightarrow SO_4^{2-} + HO^{\cdot} \quad (30)$$

Monteagudo et al. reported that diclofenac removal by sonocavitation-activated PDS was favored under acidic pH and was the same as at pH 8 [144]. Once more it was revealed the advantage of cavitation, which lowers the negative effect of pH changes. This shows applicability of the developed process in relation to real case scenario, where pH can significantly fluctuate over the time. Fan et al. also reported the similar kind of results that varying pH (3, 7, and 10) has no significant effect on the degradation of sulfamethazine by the heat-activated PDS process [142]. The less self-scavenging effect and longer life time (3–4 × 10^{-5} s) of $SO_4^{\bullet-}$ also contribute the overcoming of the pH dependency in degradation processes [6]. Thus, the usage of PDS process can be adopted directly for wastewater treatment.

Acidic pH favors the degradation of various pollutants by the HC/Fenton, HC/O_3, and HC/PDS. The solution pH of the HC-activated processes determines whether the pollutant is present in an ionic form or as a neutral molecule. Therefore, it can be stated that both pyrolytic effect and free radical attack take place when the contaminants are in the molecular state. When the operating pH is lower than the pKa of the pollutant (lower by 1.5 in respect to pKa). Comparative analysis on degradation efficiency at natural and optimal pH (2.5–3.5) conducted in laboratory scale present an appealing interest for the application in wastewater treatment.

7.2. Effect of pollutant concentration

One of the most important parameters determining the process efficiency is the initial concentration (C_0) of pollutants. An increase in reactant concentration in the system leads to the formation of products at an equilibrium state according to the thermodynamics of the reversible reaction. Increased pollutant concentration results in the formation of more oxidation products in a balanced contaminant-oxidant system. On contrary, the increased concentration of contaminants also contributes the effectiveness reduction. At higher pollutants concentration, a decrease in the degradation efficiency by cavitation can be associated with the lesser amount of •OH. This lesser amount of •OH is not sufficient to completely destroy organic contaminants. The restricted diffusion of •OH from the interfacial area of collapsing cavities minimizes the degradation efficiency, with increasing level of pollutants. Thus, the increase of degradation efficiency in HC and its combined processes has usually been observed at lower C_0 of contaminants.

Cai et al. investigated the decomposition of organic azo dye (Orange G) at various C_0 ranging from 10 to 100 mg/L using HC alone and HC/Fenton process under optimized conditions [73]. At an azo dye concentration of 20 mgL^{-1}, the degradation efficiency of 25.6% was achieved for HC alone while it was increased to 99.8% for the HC/Fenton. When C_0 of the dye was increased to 100 mgL^{-1}, the degradation efficiency was reduced rapidly to 47.3%. The degradation efficiencies were 99.8, 71.0, 52.0, and 47.3% for the HC/Fenton process at various initial dye concentrations of 20, 40, 80, and 100 mgL^{-1} after 120 min, respectively. This can be attributed to the insufficient generation of •OH to completely destroy the hydrophilic Orange G, indicating that the C_0 is an important parameter. Thus, the total amount of •OH produced are inadequate for the total number of dye molecules in the solution. As-generated •OH from the decomposition of H_2O_2 *via* the initial introduction and recombination in both gaseous and aqueous phases under HC were the driving mechanism for dye degradation.

Similarly, the effect of C_0 of reactive yellow 145 (RY 145) on the efficiency of both Fenton and sonocavitation/Fenton processes was studied by Özdemir et al. [138]. The effect of initial RY 145 concentration (50, 125, and 250 mgL^{-1}) was investigated under optimum conditions of pH 3, [Fe^{2+}] 20 mgL^{-1} and [H_2O_2] 20 mgL^{-1}, [Fe^{2+}] 20 mgL^{-1} for

the Fenton and sonocavitation/Fenton process. The sonocavitation/Fenton process achieved 95% of degradation at C_0 of 50 mg/L. While the decolorization efficiencies were significantly decreased to 75% and 71% when the C_0 were 125 and 250 mgL^{-1}, respectively. For the sole Fenton process, the degradation efficiencies were 92, 74, and 70% for the three concentrations after 60 min due to the increased concentration of the dye. Oxidizing radicals produced by the sole Fenton and sonocavitation/Fenton processes are inadequate for the decolorization of organic dye at C_0 of 125 and 250 mgL^{-1}. The increase in dye concentration resulted in reduction of decolorization in both processes. The decreasing trend of the degradation rate was because the total amount of the dye increases while the number of free radicals generated during both processes remains constant.

Several studies have shown that the optimal concentration of pollutants for the efficient degradation is dependent on the physicochemical properties of contaminants. Wang and Zhou utilized a sonocavitation-activated PDS process to degrade carbamazepine at C_0 of 5.91, 11.81, and 23.63 mgL^{-1} at a frequency of 400 kHz, pH_0 5, 50 °C, and $[PDS]_0$ 5.0 mmol L^{-1} [105]. The highest removal efficiency was achieved when C_0 of carbamazepine was 5.91 mgL^{-1}. The fast degradation occurred at a lower concentration showing that degradation was inversely proportional to C_0 of the pollutants. The degradation efficiency was decreased from 87.8 to 33.2% when C_0 was increased from 5.91 to 23.63 mgL^{-1}. High pollutant loading is detrimental because of the limited number of reaction sites and radicals.

Interestingly, Sankar et al. reported a negative synergism when sonocavitation was combined with PDS for degradation of azorubine dye-contained solution with C_0 of 20 mgL^{-1} [145]. The negative synergy was attributed to the highly sporadic nature of transient cavitation events and the scavenging of $SO_4^{\bullet-}$ by $^{\bullet}OH$ produced by US. The scavenging reaction was explained by the following equation [146].

$$HO^{\cdot} + SO_4^{\cdot-} \rightarrow HSO_4^- + \frac{1}{2}O_2 \quad (31)$$

During azorubine degradation, 46.01% of TOC was removed by UV/PDS process, while 19.05% of TOC was removed when sonocavitation-PDS. This was attributed to the non-uniform production of radicals and scavenging between $^{\bullet}OH$ and $SO_4^{\cdot-}$. In addition, the thermal activation *via* sonocavitation was hindered as the formed cavitation bubbles were not homogeneous throughout the solution. This limited the mass transfer between dye and PDS, resulting in negative synergism.

Similarly, sonocavitation-activated PDS showed different results when the C_0 of humic acid was varied between 7.5 and 30 mgL^{-1} [106]. TOC removal was declined when C_0 of humic acid was decreased, while PDS concentration, sonocavitation power, and temperature remained constant. This is because $^{\bullet}OH$ scavenged $SO_4^{\bullet-}$ at lower C_0 of humic acid. Additionally, this can be explained by the recombination of excessive $SO_4^{\bullet-}$ as shown in the following equation [144]:

$$SO_4^{\cdot-} + SO_4^{\cdot-} \rightarrow S_2O_8^{2-} \quad (32)$$

Moreover, it can be explained by the unproductive decay of $S_2O_8^{2-}$ by $^{\bullet}OH$ and thus reducing the availability of $^{\bullet}OH$ in reaction solution according to Eq. (33) [147].

$$S_2O_8^{2-} + HO^{\cdot} \rightarrow S_2O_8^{\cdot-} + HO^- \quad (33)$$

The effective collision between radicals and humic acid happens at high C_0, so the mineralization of humic acid was enhanced with the increase in C_0.

During the treatment of malachite green dye by HC/O_3, the reaction rate was decreased from 0.493 to 0.066 min^{-1} when C_0 of the dye was increased from 100 mgL^{-1} to 1000 mgL^{-1} [148]. Although the reaction rate was lower for higher dye concentration, the combination of sonocavitation and O_3 gave a positive synergy.

7.3. Effect of hydrophobicity of pollutants (characterized as K_{ow} value) on synergism

K_{ow} value of the organic compounds describes their partitioning between *n*-octanol and aqueous phase, thus defining their hydrophilic or hydrophobic character. Since the degradation processes conducted in water, the hydrophobic or hydrophilic nature of compounds defines their behavior in multiphase systems. For cavitation-based AOPs, organic compounds exhibit a preference to one of the phases – gaseous/bubble phase formed at the first stage of cavitation, gas/liquid interphase or they will tend to remain in liquid phase. More volatile and hydrophobic molecules easily diffuse into the interfacial region as well as the bubbles. High energy released during the bubble collapse is focused mainly inside of the bubble. Pyrolytic conditions in the place of collapsed bubbles promote the direct degradation of hydrophobic and volatile compounds present in this region [149]. Concentration of contaminants in the cavity–solution interface was examined by Henglein and Kormann to explain the effect of cavitation on the solutes [150]. They determined the yield of H_2O_2 in argon-saturated water samples and indicated that the hydrophobicity of contaminants is an influencing parameter.

The effect of K_{ow} value is complex and relates not only to the cavitation, but also to the side effects taking place during treatment process (sludge formation treatment reservoirs). Hydrophobic pollutants can partition on settled sludge solids and this tendency to accumulate in solids can be evaluated by using the octanol–water partition coefficient (K_{ow}). Based on evaluated physical adherence or bonding of molecules and ions on the surface of another phase the following classification was proposed [151]:

Log $K_{ow} < 2.5$ low bonding potential

Log $K_{ow} > 2.5$ and < 4.0 medium bonding potential

Log $K_{ow} > 4.0$ high bonding potential

log K_{ow} values of some contaminants along with their effect on treatment process are listed in Table 6.

The affinity towards the cavitation bubble interface depends on a larger extent of K_{ow} values. It can be observed that organic compounds with higher K_{ow} values are normally expected to have higher hydrophobicity and greater tendency to be concentrated on the bubble interface. These compounds have greater affinity to cavities than that with lower K_{ow} values. However, the tendency of some compounds with higher K_{ow} and hydrophobicity to be accumulated on the cavity region would be minimal. This can be influenced by the solution pH which affects their ionic forms in respect to pKa of the compound. The effect of cavitation on the degradation of organic compounds having higher K_{ow} values would be more pronounced due to its combination with other oxidation processes.

Randhavane and Khambete studied the degradation of chlorpyrifos pesticide by using HC [158]. Chlorpyrifos has a low water solubility (1.4 mgL^{-1}, 25 °C) and a low K_{ow} (4.7–5.3), exhibiting a moderate hydrophobic character. This hydrophobic property, which resulted in the preference gas–water interface, exhibited the advantage regarding the degradation by thermal cleavage mechanism [159]. The hydrophobic pollutants accumulated in this area will be oxidized by free radicals generated during cavitation. The optimum inlet pressure was 5 bar and the temperature 39 °C. The degradation efficiency kept increasing when solution pH was reduced to acidic. At pH 10, cavitation process obtained 75.4 % of degradation, while the degradation rate was gradually increased to 87.5 % for pH 7. At pH 3, as hydrophobic molecules are dragged into the cavitation bubbles, where they are degraded by pyrolysis, the degradation rate increases to 91.6 %. Papoutsakis et al. investigated the degradation of phenol, BPA and diuron by sonocavitation combined with Fenton [93]. Phenol was found in large quantities in the interfacial region of cavitation. It is a fairly water-soluble compound with low K_{ow} of 1.46. Thus, the hydrophilic behavior of phenol inhibits the interaction between cavitation bubble and H_2O_2. The large

Table 6
Effect of K_{ow} on degradation effectiveness under cavitation conditions.

Compound	Log K_{ow}	Conditions and findings	Ref.
Chloroform	0.84	HC exhibited low degradation rate (0.0013 min^{-1}) as the hydrophilicity reduced chloroform accumulation near the cavities.	[152]
Carbon tetrachloride	2.83	Degradation rate constant was 0.0041 min^{-1}. This was due to the higher Henry's coefficient and hydrophobicity, which promotes the accumulation of molecules near cavities or interfacial area.	[152]
Simazine	2.18	Sole sonocavitation (42 kHz) showed a low degradation rate of 0.0057 min^{-1}. It confirmed that hydrophilic compounds dispersed in the bulk solution. After addition of Au-TiO_2 (0.2 gL^{-1}) catalyst the degradation rate increased to 0.0142 min^{-1}. The synergy was achieved in higher catalyst loadings.	[153]
Atrazine	2.71	Atrazine was found resistant to O_3 oxidation due to low reaction rate at lower pH range (2–8). The synergistic effect was observed when O_3 was combined with sonocavitation at pH 10. At higher pH atrazine was exposed to radical attacks due to hydrophobic properties Thus, the degradation rate increased from 0.117 to 0.214 min^{-1} when pH was increased from 8 to 10.	[154]
Carbamazepine	2.45	Degradation was higher at pH 4 also the synergy was observed when cavitation and O_3 were combined with ξ of 2.2, sole cavitation and O_3 gave degradation rate of 0.0003 and 0.0043 min^{-1}, respectively, while HC/O_3 gave 0.0193 min^{-1}	[155]
Bisphenol A	2.2–3.84	pH influenced BPA concentration at the bubble interface. The detrimental effect was observed when pH was increased from 6 to 12. At pH 6–7 of the degradation was higher when compared with the acidic or basic conditions. There was no synergy observed at acidic or basic condition in HC/PDS.	[20]
Ibuprofen	3.97	Degradation of ibuprofen was not affected by HC under acidic or alkaline medium. pH influences the reaction mechanism apart from hydrophobicity and pollutant adsorption on bubble interface.	[156]
Diclofenac	4.51	Although higher K_{ow} value relatively the degradation under sonocavitation (585 kHz) was 0.0051 min^{-1} as the affinity towards cavities was minimal. Addition of oxidants increased the degradation rate to 0.011 min^{-1}.	[157]

amount of phenol present on the bubble liquid interface promotes the reaction with the generated free radicals during the cavitation process, because the hydrophilic molecules are easily dragged to the interface region. Therefore, these molecules are preferentially oxidized by •OH produced within the cavitation bubble. More hydrophilic intermediates of phenol degradation move from the interfacial region to the bulk solution. If most of the phenol molecules have been degraded, the bubble interface will remain free. Hydrogen peroxide will enter or be placed near the bubble without obstacles, where it may dissociate and form a new source of free radicals in the system.

Synergistic effect of sonocavitation and Fenton reaction showed the enhanced degradation of BPA (K_{ow} 3.4) and diuron (K_{ow} 2.77). The degradation of BPA attained 93% at pH 4.5 when the combined process was applied. The authors attributed this to the suppression of radical recombination and the promotion of •OH generation at acidic conditions. Hence, a greater number of •OH for the oxidation of BPA are available at the cavity-water interface. Volatile hydrophobic contaminants that dragged towards the interior of gaseous bubbles were further degraded, while the hydrophilic compounds are dissolved in the effluent. Thus, knowing K_{ow} of the pollutant, it is possible to further understand the synergy between the cavitation and other AOPs.

7.4. Treatment time

The use of combined processes with shorter treatment time has been investigated as an advancement of operating from lab-scale to raise trust among prospective users in commercial applications. The treatment time has an impact on the process efficacy and cost during treating industrial effluents. Theoretically, it is believed that the longer the treatment is, the higher the efficiency is obtained. Industrial treatment methods aim to reduce the contaminant's content in a shorter timescale. To achieve better efficiency in a shorter time, different treatment methods have been combined. An increase in the duration of cavitation process improves its effectiveness due to the increased number of passes of the treated medium through the cavitational zone.

The investigations on the synergy of combined processes have shown some simpler cumulative effects when the time duration is increased. Raut-Jadhav et al. reported that the individual oxidation process of imidacloprid resulted in a considerably small reduction in TOC. Further, TOC reduction was increased from 4.82 to 9.67 % when the processing time of HC was extended from 60 to 180 min [54]. In addition, combining HC with H_2O_2 achieved the mineralization efficiency of 26.8% in 60 min. Similar results were reported by Saxena et al. who studied the synergetic effect of HC with Fenton for treating tannery effluent [27]. They found that the HC/Fenton method can significantly reduce the dosages of H_2O_2 and $FeSO_4{\cdot}7H_2O$ (from 14.27 to 9.51 gL^{-1} and from 5 to 3 gL^{-1}, respectively) compared with the sole Fenton method, based on achieving the same TOC removal.

In most of the studies, the synergetic effect can be achieved within a short reaction time. The simultaneous application of different processes like O_3, PDS, and Fenton in combination with HC is a step in the right direction towards enhancing the process's oxidative potential due to (i) the increased production of reactive radicals (i.e., cumulative effect), and/or (ii) the beneficial process interactions (i.e., synergistic effect) with the same reaction time. The combination of various treatment processes with the HC typically has the synergetic effect within a short period. For the longer treatment time, there may be a possibility of self-scavenging due to the greater number of reactive radicals in the liquid medium. The second reason related to the presence of persistent organic compounds is not efficiently decomposed by AOPs. In this case, the prolongation of treatment time results in only a minor increase in effectiveness measured by TOC or COD analysis, thus the synergy calculated at the end is not significant. Thus, utilizing the combined process with a high synergy over short treatment time effectively degrade defined groups of compounds and proceed the effluent to further treatment process. On the other hand, the prolongation of the treatment may lead to the formation of more toxic and stable intermediates [11]. A good example is the treatment of diazinon, which can form highly stable and toxic by-product – diazoxon, when the sonocavitation, sonocavitation/Fe^{2+}, and sonocavitation/H_2O_2 treatments are prolonged [160]. From the above investigations, it can be concluded that the synergetic effect is positive for shorter periods, and when the time is prolonged toxic intermediates can be formed demanding the secondary treatment.

8. Energy and cost evaluations for synergetic processes

The operating cost of the combined HC based process mainly depends on the operation of the pump. HC reactor (HCR) setup (for non-rotational HCRs) and electrical motor (for rotational HCRs). When the cost efficiency of cavitation processes combined with AOPs is analyzed, cavitation should be considered to be a preliminary treatment in wastewater plants. This approach, by effluent pretreatment, can improve the efficiency of subsequent treatment methods such as biological treatment of activated sludge and thereby increasing the treatment plant performance by reducing toxic chemicals and derivatives. The total cost of the equipment significantly increases for cavitation-based processes.

Table 7
Results obtained by different HC-based treatment techniques dealing with wastewater.

Type of cavitating reactor	Wastewater volume (L)	Power Input (W)	Treatment time (min)	Removal efficiency (%)	Pollutant conc. (mg L^{-1})	Max. cavitation yield of unit energy input [mgJ^{-1}]	Max. cavitation yield of unit volume density energy input [$mgLJ^{-1}$]	Ref.
Liquid whistle reactor (HC)	5	3600	120	70% COD removal	9800	1.81×10^{-3}	90.74	[58]
Reactor with stator rotor assembly(HC/H_2O_2)	4	4700	20	42% COD removal	15,200	16.17×10^{-2}	646.8	[163]
Orifice plate(HC/Fenton/air)	70	5500	180	63% COD removal	12,696	1.28×10^{-2}	0.897	[75]
Orifice plate(HC)	30	2200	30	87% COD removal	42,891	64.98×10^{-2}	19.49	[164]
Venturi(HC)	15	1100	150	34% COD removal	11,648	7.05×10^{-2}	1.058	[165]
Orifice plate(HC/H_2O_2)	4	1100	30	56% TOC removal	1148	3.47×10^{-2}	0.139	[72]
Shear induced HC (Venturi type) generation (HC/H_2O_2)	2.5	370	15	45% TOC removal	176	3.17×10^{-2}	0.079	[166]
Slit or circular Venturi (HC/O_3)	20	2200	120	84 % TOC removal	8	3.03×10^{-5}	0.6×10^{-3}	[34]
Circular Venturi (HC/UV/ZnO)	22	2000	10	84 % TOC removal	24	0.12×10^{-2}	2.64×10^{-2}	[120]

Therefore, cavitation for the removal of organic pollutants may be uneconomical as an independent method. In case of sonocavitation process, this is due to the high cost of US converters and high electrical energy consumption required to attain a degradation efficiency close to that achieved in a laboratory scale. Further, additional investments required for the noise control from the cavitation processes. In case of ozonation process, the additional cost is for or the O_3 generator. For PDS and Fenton processes, the cost of chemical must be included. The advantage given by the combined processes relies on the synergistic effect obtained in cavitation conditions with other AOPs. It allows to decrease the treatment time as well as lower the total amount of external oxidant introduced into the treatment system [161,162].

Based on the concentration and type of pollutant, the energy efficiency of HCRs can be evaluated as shown in Table 7. Since AOPs are widely used in wastewater treatment, some experimental data have been collected as a starting point for the evaluation of the energy efficiency of different cavitation reactors.

The maximum cavitation yield obtained under optimum operating conditions of unit energy input is initially calculated by Eq. (34). After the pollutant volume taken into consideration, the cavitation yield of per volume density energy input is computed *via* Eq. (35) as follows:

$$Cavitation\ Yield\ (mg\ J^{-1}) = \frac{Pollu\tan t\ \deg raded}{Power\ of\ pump\ x\ time} \quad (34)$$

$$Cavitation\ Yield\ \left(mg\ L\ J^{-1}\right) = \frac{Pollu\tan t\ \deg rade}{(Power\ of\ pump\ x\ time)\ /\ intial\ vo}$$

Chiknala et al. reported the efficacy of industrial wastewater treatment by a liquid whistle reactor combined with Fenton process [58]. In this process, the COD of complex phenolic compounds (42000 mg/L) was reduced up to 85% with the cavitational yield of 1.81×10^{-3} mg J^{-1}. They have reported that HC in combination with Fenton process can be used efficiently for the pretreatment of effluent. Badve et al. reported a COD reduction of 49% during the treatment of effluents containing the high amounts of VOCs with a cavitational yield of 16.17×10^{-2} mg J^{-1} [163]. The addition of H_2O_2 to the HCR increased the cavitational yield and the oxidation of VOCs.

Joshi and Gogate investigated the treatment of industrial wastewater with an initial COD of 100 mgL^{-1} by a pilot-scale plant with a working capacity of 70 L [75]. They observed that the combination of Fenton with HC enhanced the COD removal 42% to 63% in 180 min with a cavitational yield of 1.28×10^{-2} mg J^{-1}. They also emphasized on the addition of O_2 from an external source which increased the cavitation yield, resulting in a greater COD removal within 180 min. Montusiewicz et al. concluded that the repeated dilution or mixing of municipal wastewater increased the solubility of contaminants (carbohydrates, monosaccharides). This diluted sample going through HC gained 87 % of COD removal [164]. The physical effects increased a cavitational yield to 64.98×10^{-2} mg J^{-1}. The bio-methanated distillery wastewater having COD of 35,000 mgL^{-1} was treated with HC process [165]. A 25% dilution of wastewater increased the COD removal efficiency to 34% with the cavitational yield of 7.05×10^{-2} mg J^{-1}. Patil and Gogate examined the degradation of complex organic contaminant methyl parathion [72]. The combination of H_2O_2 with cavitation yielded a TOC removal of 56.4%. The cavitational yield was about 3.17×10^{-2} mg J^{-1}. Treatment of pharmaceuticals by HC in combination with H_2O_2 resulted in a 45% TOC removal [166]. Rajoriya et al. observed a TOC removal efficiency of 84% for cationic azo dyes with the cavitational yield of 0.6×10^{-3} mg L J^{-1} [34]. The synthetic dye solutions were treated by the HC with a lower cavitational yield in the presence of O_3. While Çaliskan et al. reported a cavitational yield of 2.64×10^{-2} mg L J^{-1} was required for achieving a TOC removal of 84% for industrial textile wastewater by using the combination of H_2O_2, ZnO, and HC [120].

A combination of HC and AOPs guarantees the maximum cavitation output from the unit power supply. If the impact of water volume is considered, cavitation with the addition of H_2O_2, Fenton's reagent, and PDS can be distinguished. The energy distribution is relatively uniform in HCRs. Furthermore, HC enables continuous operation and the amount of pollutant being treated is larger. Overall, there are certain advantages of HC in large scale operation and industrial applications. This process should be combined with AOPs to improve the degradation efficiency.

9. Future suggestions and recommendations

As discussed, the development of cost-effective treatment methods can be obtained by coupling HC with AOPs. These hybrid processes are promising methods to enhance the deterioration of recalcitrant pollutants for their compatibilities with the environment. Synergistic effect enhances the mass transport of contaminant owing to physical (shock waves, cavitating microjet) and chemical effects of cavitation. It reduces pollutant aggregation and increases oxidation of contaminants, eliminating the formation of intermediates. Despite the high capital cost, HC-based hybrid processes allow to decrease the energy and cost

required for complete mineralization. Following are the suggestions for future studies to further improve the treatment technology.

i) The cavitation number and number of operating parameters should be optimized for each HCR. Details regarding cavitating device should be provided to allow researchers to analyze reactor's structure and scale-up processes. The variety of equipment has to be developed with optimized operating conditions to obtain the expected yield.

(ii) To attain favorable results, standardized devices should be utilized. Mainly, commercially available parts should be the first choice. To investigate the effect of such factors on bubble dynamics and degradation, the design and production of devices with different flow fields, turbulence characteristics, and geometrical parameters are necessary.

(iii) The new equipment used to build the better HCR devices must be investigated. Geometry of HCRs must be properly designed to improve cavitational activity. The theoretical design strategies should be in relation with experimental results.

(iv) Multicomponent solutions experiments must be conducted. The reaction rate and products to characterize and optimize the degradation process should be detected. Interaction between the various components should be considered in order to produce reproductive results.

(v) To evaluate the impact of physicochemical properties on degradation process, a large number of substrates should be used. The conversion should correlate with properties, like vapor pressure, solubility, viscosity, surface tension, and density.

(vi) The role of sequential addition of oxidants (Fenton, PDS, O_3) must be optimized to reduce the time and cost of the process. The loadings have to be developed and studied in pilot scale as preliminary studies should eradicate the sludge formation during the process.

(vii) Further studies should reveal reaction pathways comparing to typical AOPs, including toxicity of formed by-products. This is highly important as several interesting groups of by-products were identified in cavitation-based AOPs.

10. Conclusion

In this review, we summarized various aspects of HC-based AOPs which were successfully utilized for the degradation of recalcitrant organic contaminants. Analysis of data presented in this review allowed to postulate several important bullet points that summarized as guidelines for future researches:

(1) Degradation of pollutants in HC process increases with an increase in the flow velocity (i.e. with pressure at the inlet) till the optimum value. The best parameter to characterize this dependency (it is related to flowrate and diameter of constriction) is the cavitation number. In this convention C_v of 0.1–0.35 seems to be optimal in most cases. Beyond this values range, the degradation effectiveness decreases due to the super-cavitation and reduction in generation of cavities ($C_v \sim 0$).

(2) The optimum inlet pressure in HC must be investigated as it affects the bubble formation and collapse intensity inside the reactor. The optimum operating pressure is also dependent on the geometry of HCRs.

(3) The synergism should be evaluated for few points of time during the degradation and based mostly on reaction rate constant (k) rather than the final TOC or COD removal. However, this data should be reported together to, firstly, indicate the synergism and, secondly, to show high/total reduction of pollution load on the basis of COD or TOC.

(4) It is recommended to operate at the actual temperature of the wastewater to reduce the operating cost of the treatment method. The optimum operating temperature must be studied since the temperature of the medium affects the generation of free radicals. In HC/PDS, the increase in temperature to 30 to 40 °C favors the rise in generation of $SO_4^{\bullet-}$, thus increasing the degradation kinetics.

(5) Generally, acidic conditions favor the HC-mediated treatment methods. In case of pH adjustment, the cost of chemicals must be included along with effectiveness and process kinetics to determine optimal value.

(6) Properties of pollutants such as concentration, viscosity, and surface tension in water need to be investigated. An increase in C_0 decreases the pollutant removal rate. An increase in viscosity, regardless of whether fluids are Newtonian or non-Newtonian, reduces the efficiency of cavitation due to decreased cavitational effect of bubble growth and collapse.

(7) Under optimized operating parameters of HC and oxidant/catalyst loadings, hybrid HC/AOPs processes show excellent oxidation capacity due to the increased generation of reactive radicals and preclude the drawbacks associated with partial activation, sludge formation, mass transfer resistance.

(8) Hydrodynamic cavitation proved to be synergistic in all types of reviewed hybrid processes. In most of the cases values of ξ are in the range of 1,5–4,5 or even 6 (in case of H_2O_2). This indicates that every AOP can be effectively assisted by cavitation phenomenon resulting in 150–450% increase of rate constant values. In few cases ξ values were exceeding 10 (or even 25), however the authors didn't try to analyze or explain in details what could cause such unusual process improvements. On the basis of materials present in such papers, it is hard to make any additional conclusions.

(9) High ξ values of HC/H_2O_2 process prove that cheap and commonly available H_2O_2 (but not very effective when used alone) in combination with cavitation can compete with other AOPs in effective degradation of many water pollutants. Secondly, cavitation allows to expand the applicable range of pH values even to strongly basic environment.

(10) In all cases ξ values should be related to obtained final degradation. Often high synergism does not mean a total degradation. On the other hand, further confirmation of process effectiveness by mineralization studies should be accompanied to fully evaluate the treatment effect.

The possibility of coupling several AOPs with HC is still an open case. It was proved that very high synergism can be obtained in several processes. As the synergistic character of hybrid processes has been already proved, researchers face big challenges to perform further studies in this field. It relates to the demand to study several aspects of the developed process. The most interesting is the degradation mechanism which can include direct cavitational effect as well as direct oxidation and several AOPs related radical reactions. In case of gaseous oxidants, such as O_2 or O_3, it was proved that HC – as a must – generates an overpressure region before the constriction, which makes perfect conditions to increase the solubility of gaseous oxidants. The alternative aspect of studies relates to the effect of dissolved gas on cavitation events. Next, heterogeneous catalytic processes must be discussed in relation to oxidants activation but also in relation to cavitation. Several catalysts were proved to have sonocatalytic properties increasing a number of cavitation events in case of HC *via* simple particle effect on formation and collapse of bubbles. Effect of inorganic ions on hybrid processes must include the fate of these ions (especially anions) as cavitation conditions sufficient to form organic by-products. This must include also the effect of nitrogen fixation as nitrates, as several papers reported the formation of nitro-derivatives of degraded pollutants. This also relates to risk assessment on the basis of biotoxicity of the treated effluents. Finally, studies on scaling up of developed processes are scarce. This would give new insights on the effectiveness of designed HC-based processes to be implemented in real industrial practice.

Listed aspects are the most important points that should be taken into consideration for further studies on hybrid processes. Only our imagination coupled with knowledge on the topic limits the spectrum of interesting features that can be placed in future papers on HC-based hybrid AOPs.

Declaration of Competing Interest

The authors declare that they have no known competing financial interests or personal relationships that could have appeared to influence the work reported in this paper.

Acknowledgements

The authors gratefully acknowledge financial support from the National Science Centre, Warsaw, Poland for project OPUS nr UMO-2017/25/B/ST8/01364 and the National Natural Science Foundation of China (grant nos. 51906125). Dr Shirish Sonawane acknowledge to the Ulam program of the Polish National Agency for Academic Exchange (NAWA) (Grant number:PPN/ULM/2020/1/00037/U/00001).

References

[1] A. Rezaee, H. Masoumbeigi, R.D.C. Soltani, A.R. Khataee, S. Hashemiyan, Photocatalytic decolorization of methylene blue using immobilized ZnO nanoparticles prepared by solution combustion method, Desalin. Water Treat. 44 (1–3) (2012) 174–179, https://doi.org/10.1080/19443994.2012.691700.

[2] R. Darvishi Cheshmeh Soltani, A.R. Khataee, M. Mashayekhi, Photocatalytic degradation of a textile dye in aqueous phase over ZnO nanoparticles embedded in biosilica nanobiostructure, Desalin. Water Treat. 57 (29) (2016) 13494–13504, https://doi.org/10.1080/19443994.2015.1058193.

[3] R. Darvishi Cheshmeh Soltani, M. Mashayekhi, Decomposition of ibuprofen in water via an electrochemical process with nano-sized carbon black-coated carbon cloth as oxygen-permeable cathode integrated with ultrasound, Chemosphere. 194 (2018) 471–480, https://doi.org/10.1016/j.chemosphere.2017.12.033.

[4] R. Darvishi Cheshmeh Soltani, M. Mashayekhi, S. Jorfi, A. Khataee, M.-J. Ghanadzadeh, M. Sillanpää, Implementation of martite nanoparticles prepared through planetary ball milling as a heterogeneous activator of oxone for degradation of tetracycline antibiotic: Ultrasound and peroxy-enhancement, Chemosphere. 210 (2018) 699–708, https://doi.org/10.1016/j.chemosphere.2018.07.077.

[5] S. Giannakis, F.A. Gamarra Vives, D. Grandjean, A. Magnet, L.F. De Alencastro, C. Pulgarin, Effect of advanced oxidation processes on the micropollutants and the effluent organic matter contained in municipal wastewater previously treated by three different secondary methods, Water Res. 84 (2015) 295–306, https://doi.org/10.1016/j.watres.2015.07.030.

[6] R. Dewil, D. Mantzavinos, I. Poulios, M.A. Rodrigo, New perspectives for advanced oxidation processes, J. Environ. Manage. 195 (2017) 93–99, https://doi.org/10.1016/j.jenvman.2017.04.010.

[7] X. Sun, J. Liu, L.I. Ji, G. Wang, S. Zhao, J.Y. Yoon, S. Chen, A review on hydrodynamic cavitation disinfection: The current state of knowledge, Sci. Total Environ. 737 (2020) 139606, https://doi.org/10.1016/j.scitotenv.2020.139606.

[8] X. Sun, X. Xuan, Y. Song, X. Jia, L.i. Ji, S. Zhao, J. Yong Yoon, S. Chen, J. Liu, G. Wang, Experimental and numerical studies on the cavitation in an advanced rotational hydrodynamic cavitation reactor for water treatment, Ultrason. Sonochem. 70 (2021) 105311, https://doi.org/10.1016/j.ultsonch.2020.105311.

[9] M. Mehrjouei, S. Müller, D. Möller, A review on photocatalytic ozonation used for the treatment of water and wastewater, Chem. Eng. J. 263 (2015) 209–219, https://doi.org/10.1016/j.cej.2014.10.112.

[10] A. Asghar, A.A.A. Raman, W.M.A.W. Daud, Advanced oxidation processes for in-situ production of hydrogen peroxide/hydroxyl radical for textile wastewater treatment: A review, J. Clean. Prod. 87 (2015) 826–838, https://doi.org/10.1016/j.jclepro.2014.09.010.

[11] M. Gągol, A. Przyjazny, G. Boczkaj, Wastewater treatment by means of advanced oxidation processes based on cavitation – A review, Chem. Eng. J. 338 (2018) 599–627, https://doi.org/10.1016/J.CEJ.2018.01.049.

[12] Q. Wang, Y.E. Cao, H. Zeng, Y. Liang, J. Ma, X. Lu, Ultrasound-enhanced zero-valent copper activation of persulfate for the degradation of bisphenol AF, Chem. Eng. J. 378 (2019) 122143, https://doi.org/10.1016/j.cej.2019.122143.

[13] M. Gągol, E. Cako, K. Fedorov, R.D.C. Soltani, A. Przyjazny, G. Boczkaj, Hydrodynamic cavitation based advanced oxidation processes: Studies on specific effects of inorganic acids on the degradation effectiveness of organic pollutants, J. Mol. Liq. 307 (2020) 113002, https://doi.org/10.1016/j.molliq.2020.113002.

[14] G. Boczkaj, M. Gągol, M. Klein, A. Przyjazny, Effective method of treatment of effluents from production of bitumens under basic pH conditions using hydrodynamic cavitation aided by external oxidants, Ultrason. Sonochem. 40 (2018) 969–979, https://doi.org/10.1016/j.ultsonch.2017.08.032.

[15] X. Sun, W. You, X. Xuan, L.I. Ji, X. Xu, G. Wang, S. Zhao, G. Boczkaj, J.Y. Yoon, S. Chen, Effect of the cavitation generation unit structure on the performance of an advanced hydrodynamic cavitation reactor for process intensifications, Chem. Eng. J. 412 (2021) 128600, https://doi.org/10.1016/j.cej.2021.128600.

[16] X. Sun, X. Xuan, L.I. Ji, S. Chen, J. Liu, S. Zhao, S. Park, J.Y. Yoon, A.S. Om, A novel continuous hydrodynamic cavitation technology for the inactivation of pathogens in milk, Ultrason. Sonochem. 71 (2021) 105382, https://doi.org/10.1016/j.ultsonch.2020.105382.

[17] M. Gągol, A. Przyjazny, G. Boczkaj, Effective method of treatment of industrial effluents under basic pH conditions using acoustic cavitation – A comprehensive comparison with hydrodynamic cavitation processes, Chem. Eng. Process. - Process Intensif. 128 (2018) 103–113, https://doi.org/10.1016/J.CEP.2018.04.010.

[18] M. Čehovin, A. Medic, J. Scheideler, J. Mielcke, A. Ried, B. Komparc, A. Žgajnar Gotvajn, Hydrodynamic cavitation in combination with the ozone, hydrogen peroxide and the UV-based advanced oxidation processes for the removal of natural organic matter from drinking water, Ultrason. Sonochem. 37 (2017) 394–404, https://doi.org/10.1016/j.ultsonch.2017.01.036.

[19] Z. Wu, F.J. Yuste-Córdoba, P. Cintas, Z. Wu, L. Boffa, S. Mantegna, G. Cravotto, Effects of ultrasonic and hydrodynamic cavitation on the treatment of cork wastewater by flocculation and fenton processes, Ultrason. Sonochem. 40 (2018) 3–8, https://doi.org/10.1016/j.ultsonch.2017.04.016.

[20] J. Choi, M. Cui, Y. Lee, J. Kim, Y. Son, J. Khim, Hydrodynamic cavitation and activated persulfate oxidation for degradation of bisphenol A: Kinetics and mechanism, Chem. Eng. J. 338 (2018) 323–332, https://doi.org/10.1016/J.CEJ.2018.01.018.

[21] E. Hu, X. Wu, S. Shang, X.M. Tao, S.X. Jiang, L. Gan, Catalytic ozonation of simulated textile dyeing wastewater using mesoporous carbon aerogel supported copper oxide catalyst, J. Clean. Prod. 112 (2016) 4710–4718, https://doi.org/10.1016/j.jclepro.2015.06.127.

[22] K.B. Orhon, A.K. Orhon, F.B. Dilek, U. Yetis, Triclosan removal from surface water by ozonation - Kinetics and by-products formation, J. Environ. Manage. 204 (2017) 327–336, https://doi.org/10.1016/j.jenvman.2017.09.025.

[23] C. Rodríguez, J.I. Lombraña, A. de Luis, J. Sanz, Oxidizing efficiency analysis of an ozonation process to degrade the dye rhodamine 6G, J. Chem. Technol. Biotechnol. 92 (3) (2017) 674–683, https://doi.org/10.1002/jctb.5051.

[24] A. de Luis, J.I. Lombraña, pH-Based strategies for an efficient addition of h2o2 during ozonation to improve the mineralisation of two contaminants with different degradation resistances, Water, Air, Soil Pollut. 229 (2018) 372, https://doi.org/10.1007/s11270-018-4014-8.

[25] M. Gągol, A. Przyjazny, G. Boczkaj, Highly effective degradation of selected groups of organic compounds by cavitation based AOPs under basic pH conditions, Ultrason. Sonochem. 45 (2018) 257–266, https://doi.org/10.1016/J.ULTSONCH.2018.03.013.

[26] A.J. Barik, P.R. Gogate, Degradation of 4-chloro 2-aminophenol using a novel combined process based on hydrodynamic cavitation, UV photolysis and ozone, Ultrason. Sonochem. 30 (2016) 70–78, https://doi.org/10.1016/j.ultsonch.2015.11.007.

[27] S. Saxena, V.K. Saharan, S. George, Enhanced synergistic degradation efficiency using hybrid hydrodynamic cavitation for treatment of tannery waste effluent, J. Clean. Prod. 198 (2018) 1406–1421, https://doi.org/10.1016/j.jclepro.2018.07.135.

[28] P.R. Gogate, P.N. Patil, Combined treatment technology based on synergism between hydrodynamic cavitation and advanced oxidation processes, Ultrason. Sonochem. 25 (2015) 60–69, https://doi.org/10.1016/J.ULTSONCH.2014.08.016.

[29] P. Thanekar, P.R. Gogate, Improved processes involving hydrodynamic cavitation and oxidants for treatment of real industrial effluent, Sep. Purif. Technol. 239 (2020) 116563, https://doi.org/10.1016/j.seppur.2020.116563.

[30] S. Rajoriya, S. Bargole, S. George, V.K. Saharan, Treatment of textile dyeing industry effluent using hydrodynamic cavitation in combination with advanced oxidation reagents, J. Hazard. Mater. 344 (2018) 1109–1115, https://doi.org/10.1016/j.jhazmat.2017.12.005.

[31] A.J. Barik, P.R. Gogate, Hybrid treatment strategies for 2,4,6-trichlorophenol degradation based on combination of hydrodynamic cavitation and AOPs, Ultrason. Sonochem. 40 (2018) 383–394, https://doi.org/10.1016/j.ultsonch.2017.07.029.

[32] R.H. Jawale, P.R. Gogate, Novel approaches based on hydrodynamic cavitation for treatment of wastewater containing potassium thiocyanate, Ultrason. Sonochem. 52 (2019) 214–223, https://doi.org/10.1016/j.ultsonch.2018.11.019.

[33] Z. Wu, M. Franke, B. Ondruschka, Y. Zhang, Y. Ren, P. Braeutigam, W. Wang, Enhanced effect of suction-cavitation on the ozonation of phenol, J. Hazard. Mater. 190 (1–3) (2011) 375–380, https://doi.org/10.1016/j.jhazmat.2011.03.054.

[34] S. Rajoriya, S. Bargole, V.K. Saharan, Degradation of a cationic dye (Rhodamine 6G) using hydrodynamic cavitation coupled with other oxidative agents: Reaction mechanism and pathway, Ultrason. Sonochem. 34 (2017) 183–194, https://doi.org/10.1016/j.ultsonch.2016.05.028.

[35] S. Raut-Jadhav, M.P. Badve, D.V. Pinjari, D.R. Saini, S.H. Sonawane, A.B. Pandit, Treatment of the pesticide industry effluent using hydrodynamic cavitation and its combination with process intensifying additives (H 2 O 2 and ozone), Chem. Eng. J. 295 (2016) 326–335, https://doi.org/10.1016/j.cej.2016.03.019.

[36] E. Cako, K.D. Gunasekaran, R.D. Cheshmeh Soltani, G. Boczkaj, Ultrafast degradation of brilliant cresyl blue under hydrodynamic cavitation based advanced oxidation processes (AOPs), Water Resour, Ind. 24 (2020) 100134, https://doi.org/10.1016/j.wri.2020.100134.

[37] P. Thanekar, P. Murugesan, P.R. Gogate, Improvement in biological oxidation process for the removal of dichlorvos from aqueous solutions using pretreatment based on Hydrodynamic Cavitation, J. Water Process Eng. 23 (2018) 20–26, https://doi.org/10.1016/j.jwpe.2018.03.004.

[38] A. Mukherjee, A. Mullick, R. Teja, P. Vadthya, A. Roy, S. Moulik, Performance and energetic analysis of hydrodynamic cavitation and potential integration with existing advanced oxidation processes: A case study for real life greywater treatment, Ultrason. Sonochem. 66 (2020) 105116, https://doi.org/10.1016/j.ultsonch.2020.105116.

[39] P. Thanekar, S. Garg, P.R. Gogate, Hybrid treatment strategies based on hydrodynamic cavitation, advanced oxidation processes, and aerobic oxidation for efficient removal of naproxen, Ind. Eng. Chem. Res. 59 (9) (2020) 4058–4070, https://doi.org/10.1021/acs.iecr.9b01395.
[40] I. Ofori, S. Maddila, J. Lin, S.B. Jonnalagadda, Ozone initiated inactivation of Escherichia coli and Staphylococcus aureus in water: Influence of selected organic solvents prevalent in wastewaters, Chemosphere. 206 (2018) 43–50, https://doi.org/10.1016/j.chemosphere.2018.04.164.
[41] L.K. Weavers, F.H. Ling, M.R. Hoffmann, Aromatic compound degradation in water using a combination of sonolysis and ozonolysis, Environ. Sci. Technol. 32 (18) (1998) 2727–2733, https://doi.org/10.1021/es970675a.
[42] E.M. Aieta, K.M. Reagan, J.S. Lang, L. McReynolds, J.-W. Kang, W.H. Glaze, Advanced oxidation processes for treating groundwater contaminated with tce and pce: pilot-scale evaluations, J. AWWA. 80 (5) (1988) 64–72, https://doi.org/10.1002/j.1551-8833.1988.tb03039.x.
[43] G. Boczkaj, A. Fernandes, Wastewater treatment by means of advanced oxidation processes at basic pH conditions: A review, Chem. Eng. J. 320 (2017) 608–633, https://doi.org/10.1016/J.CEJ.2017.03.084.
[44] P. Saritha, C. Aparna, V. Himabindu, Y. Anjaneyulu, Comparison of various advanced oxidation processes for the degradation of 4-chloro-2 nitrophenol, J. Hazard. Mater. 149 (3) (2007) 609–614.
[45] K.W. Jung, S.Y. Lee, Y.J. Lee, J.W. Choi, Ultrasound-assisted heterogeneous Fenton-like process for bisphenol A removal at neutral pH using hierarchically structured manganese dioxide/biochar nanocomposites as catalysts, Ultrason. Sonochem. 57 (2019) 22–28, https://doi.org/10.1016/J.ULTSONCH.2019.04.039.
[46] S. Baradaran, M.T. Sadeghi, Coomassie Brilliant Blue (CBB) degradation using hydrodynamic cavitation, hydrogen peroxide and activated persulfate (HC-H2O2-KPS) combined process, Chem. Eng. Process. - Process Intensif. 145 (2019) 107674, https://doi.org/10.1016/j.cep.2019.107674.
[47] P. Thanekar, P.R. Gogate, Combined hydrodynamic cavitation based processes as an efficient treatment option for real industrial effluent, Ultrason. Sonochem. 53 (2019) 202–213, https://doi.org/10.1016/J.ULTSONCH.2019.01.007.
[48] S. Rajoriya, S. Bargole, V.K. Saharan, Degradation of reactive blue 13 using hydrodynamic cavitation: Effect of geometrical parameters and different oxidizing additives, Ultrason. Sonochem. 37 (2017) 192–202, https://doi.org/10.1016/j.ultsonch.2017.01.005.
[49] M.M. Gore, V.K. Saharan, D.V. Pinjari, P.V. Chavan, A.B. Pandit, Degradation of reactive orange 4 dye using hydrodynamic cavitation based hybrid techniques, Ultrason. Sonochem. 21 (3) (2014) 1075–1082, https://doi.org/10.1016/j.ultsonch.2013.11.015.
[50] A. Mukherjee, A. Mullick, P. Vadthya, S. Moulik, A. Roy, Surfactant degradation using hydrodynamic cavitation based hybrid advanced oxidation technology: A techno economic feasibility study, Chem. Eng. J. 398 (2020) 125599, https://doi.org/10.1016/j.cej.2020.125599.
[51] S. Raut-Jadhav, D. Saini, S. Sonawane, A. Pandit, Effect of process intensifying parameters on the hydrodynamic cavitation based degradation of commercial pesticide (methomyl) in the aqueous solution, Ultrason. Sonochem. 28 (2016) 283–293, https://doi.org/10.1016/J.ULTSONCH.2015.08.004.
[52] P.N. Patil, S.D. Bote, P.R. Gogate, Degradation of imidacloprid using combined advanced oxidation processes based on hydrodynamic cavitation, Ultrason. Sonochem. 21 (5) (2014) 1770–1777, https://doi.org/10.1016/j.ultsonch.2014.02.024.
[53] M.S. Kumar, S.H. Sonawane, A.B. Pandit, Degradation of methylene blue dye in aqueous solution using hydrodynamic cavitation based hybrid advanced oxidation processes, Chem. Eng. Process. Process Intensif. 122 (2017) 288–295, https://doi.org/10.1016/J.CEP.2017.09.009.
[54] S. Raut-Jadhav, V.K. Saharan, D. Pinjari, S. Sonawane, D. Saini, A. Pandit, Synergetic effect of combination of AOP's (hydrodynamic cavitation and H2O2) on the degradation of neonicotinoid class of insecticide, J. Hazard. Mater. 261 (2013) 139–147, https://doi.org/10.1016/J.JHAZMAT.2013.07.012.
[55] M.S. Kumar, S.H. Sonawane, B.A. Bhanvase, B. Bethi, Treatment of ternary dye wastewater by hydrodynamic cavitation combined with other advanced oxidation processes (AOP's), J. Water Process Eng. 23 (2018) 250–256, https://doi.org/10.1016/j.jwpe.2018.04.004.
[56] M. Zupanc, T. Kosjek, M. Petkovšek, M. Dular, B. Kompare, B. Širok, Ž. Blažeka, E. Heath, Removal of pharmaceuticals from wastewater by biological processes, hydrodynamic cavitation and UV treatment, Ultrason. Sonochem. 20 (4) (2013) 1104–1112.
[57] A.G. Chakinala, D.H. Bremner, P.R. Gogate, K.-C. Namkung, A.E. Burgess, Multivariate analysis of phenol mineralisation by combined hydrodynamic cavitation and heterogeneous advanced fenton processing, Appl. Catal. B Environ. 78 (1–2) (2008) 11–18, https://doi.org/10.1016/j.apcatb.2007.08.012.
[58] A.G. Chakinala, P.R. Gogate, A.E. Burgess, D.H. Bremner, Treatment of industrial wastewater effluents using hydrodynamic cavitation and the advanced fenton process, Ultrason. Sonochem. 15 (1) (2008) 49–54, https://doi.org/10.1016/j.ultsonch.2007.01.003.
[59] J. Wang, X. Wang, P. Guo, J. Yu, Degradation of reactive brilliant red K-2BP in aqueous solution using swirling jet-induced cavitation combined with H2O2, Ultrason. Sonochem. 18 (2) (2011) 494–500, https://doi.org/10.1016/j.ultsonch.2010.08.006.
[60] A. Asghar, A.A. Abdul Raman, W.M.A. Wan Daud, Advanced oxidation processes for in-situ production of hydrogen peroxide/hydroxyl radical for textile wastewater treatment: a review, J. Clean. Prod. 87 (2015) 826–838, https://doi.org/10.1016/j.jclepro.2014.09.010.
[61] D. Huang, C. Hu, G. Zeng, M. Cheng, P. Xu, X. Gong, R. Wang, W. Xue, Combination of fenton processes and biotreatment for wastewater treatment and soil remediation, Sci. Total Environ. 574 (2017) 1599–1610, https://doi.org/10.1016/j.scitotenv.2016.08.199.
[62] L. Li, C. Lai, F. Huang, M. Cheng, G. Zeng, D. Huang, B. Li, S. Liu, M.M. Zhang, L. Qin, M. Li, J. He, Y. Zhang, L. Chen, Degradation of naphthalene with magnetic bio-char activate hydrogen peroxide: Synergism of bio-char and Fe–Mn binary oxides, Water Res. 160 (2019) 238–248, https://doi.org/10.1016/j.watres.2019.05.081.
[63] J.H. Fenton, Oxidationoftartaricacidinpresenceof iron, J. Chem. Soc. Trans. 65 (1894) 899–910.
[64] L. Chu, J. Wang, J. Dong, H. Liu, X. Sun, Treatment of coking wastewater by an advanced Fenton oxidation process using iron powder and hydrogen peroxide, Chemosphere. 86 (4) (2012) 409–414, https://doi.org/10.1016/j.chemosphere.2011.09.007.
[65] B. Bethi, S.H. Sonawane, B.A. Bhanvase, S.P. Gumfekar, Nanomaterials-based advanced oxidation processes for wastewater treatment: A review, Chem. Eng. Process. Process Intensif. 109 (2016) 178–189, https://doi.org/10.1016/j.cep.2016.08.016.
[66] S. Garcia-Segura, L.M. Bellotindos, Y.H. Huang, E. Brillas, M.C. Lu, Fluidized-bed fenton process as alternative wastewater treatment technology—A review, J. Taiwan Inst. Chem. Eng. 67 (2016) 211–225, https://doi.org/10.1016/j.jtice.2016.07.021.
[67] Y. Zhu, R. Zhu, Y. Xi, J. Zhu, G. Zhu, H. He, Strategies for enhancing the heterogeneous fenton catalytic reactivity: A review, Appl. Catal. B Environ. 255 (2019) 117739, https://doi.org/10.1016/j.apcatb.2019.05.041.
[68] A.G. Chakinala, P.R. Gogate, A.E. Burgess, D.H. Bremner, Industrial wastewater treatment using hydrodynamic cavitation and heterogeneous advanced fenton processing, Chem. Eng. J. 152 (2–3) (2009) 498–502, https://doi.org/10.1016/j.cej.2009.05.018.
[69] A.A. Pradhan, P.R. Gogate, Removal of p-nitrophenol using hydrodynamic cavitation and fenton chemistry at pilot scale operation, Chem. Eng. J. 156 (1) (2010) 77–82, https://doi.org/10.1016/j.cej.2009.09.042.
[70] M.V. Bagal, P.R. Gogate, Wastewater treatment using hybrid treatment schemes based on cavitation and fenton chemistry: A review, Ultrason. Sonochem. 21 (1) (2014) 1–14, https://doi.org/10.1016/j.ultsonch.2013.07.009.
[71] R.K. Joshi, P.R. Gogate, Degradation of dichlorvos using hydrodynamic cavitation based treatment strategies, Ultrason. Sonochem. 19 (3) (2012) 532–539, https://doi.org/10.1016/j.ultsonch.2011.11.005.
[72] P.N. Patil, P.R. Gogate, Degradation of methyl parathion using hydrodynamic cavitation: Effect of operating parameters and intensification using additives, Sep. Purif. Technol. 95 (2012) 172–179, https://doi.org/10.1016/j.seppur.2012.04.019.
[73] M. Cai, J. Su, Y. Zhu, X. Wei, M. Jin, H. Zhang, C. Dong, Z. Wei, Decolorization of azo dyes Orange G using hydrodynamic cavitation coupled with heterogeneous Fenton process, Ultrason. Sonochem. 28 (2016) 302–310, https://doi.org/10.1016/j.ultsonch.2015.08.001.
[74] J. Wang, Y. Guo, P. Guo, J. Yu, W. Guo, X. Wang, Degradation of reactive brilliant red K-2BP in water using a combination of swirling jet-induced cavitation and fenton process, Sep. Purif. Technol. 130 (2014) 1–6, https://doi.org/10.1016/j.seppur.2014.04.020.
[75] S.M. Joshi, P.R. Gogate, Intensification of industrial wastewater treatment using hydrodynamic cavitation combined with advanced oxidation at operating capacity of 70 L, Ultrason. Sonochem. 52 (2019) 375–381, https://doi.org/10.1016/j.ultsonch.2018.12.016.
[76] V. Innocenzi, M. Prisciandaro, M. Centofanti, F. Vegliò, Comparison of performances of hydrodynamic cavitation in combined treatments based on hybrid induced advanced Fenton process for degradation of azo-dyes, J. Environ. Chem. Eng. 7 (3) (2019) 103171, https://doi.org/10.1016/j.jece:2019.103171.
[77] Z. Askarniya, M.-T. Sadeghi, S. Baradaran, Decolorization of Congo red via hydrodynamic cavitation in combination with fenton's reagent, Chem. Eng. Process. - Process Intensif. 150 (2020) 107874, https://doi.org/10.1016/j.cep.2020.107874.
[78] S. Raut-Jadhav, V.K. Saharan, D.V. Pinjari, D.R. Saini, S.H. Sonawane, A.B. Pandit, Intensification of degradation of imidacloprid in aqueous solutions by combination of hydrodynamic cavitation with various advanced oxidation processes (AOPs), J. Environ. Chem. Eng. 1 (4) (2013) 850–857.
[79] M.V. Bagal, P.R. Gogate, Degradation of 2,4-dinitrophenol using a combination of hydrodynamic cavitation, chemical and advanced oxidation processes, Ultrason. Sonochem. 20 (5) (2013) 1226–1235, https://doi.org/10.1016/j.ultsonch.2013.02.004.
[80] E.G. Garrido-Ramírez, B.K.G. Theng, M.L. Mora, Clays and oxide minerals as catalysts and nanocatalysts in Fenton-like reactions - A review, Appl. Clay Sci. 47 (3–4) (2010) 182–192, https://doi.org/10.1016/j.clay.2009.11.044.
[81] S. Rahim Pouran, A.A. Abdul Raman, W.M.A. Wan Daud, Review on the application of modified iron oxides as heterogeneous catalysts in Fenton reactions, J. Clean. Prod. 64 (2014) 24–35, https://doi.org/10.1016/j.jclepro.2013.09.013.
[82] D. Spuhler, J. Andrés Rengifo-Herrera, C. Pulgarin, The effect of Fe2+, Fe3+, H2O2 and the photo-Fenton reagent at near neutral pH on the solar disinfection (SODIS) at low temperatures of water containing escherichia coli K12, Appl. Catal. B Environ. 96 (1–2) (2010) 126–141, https://doi.org/10.1016/j.apcatb.2010.02.010.
[83] W. Brack, V. Dulio, M. Ågerstrand, I. Allan, R. Altenburger, M. Brinkmann, D. Bunke, R.M. Burgess, I. Cousins, B.I. Escher, F.J. Hernández, L.M. Hewitt, K. Hilscherová, J. Hollender, H. Hollert, R. Kase, B. Klauer, C. Lindim, D.L. Herráez, C. Miège, J. Munthe, S. O'Toole, L. Posthuma, H. Rüdel, R.B. Schäfer, M. Sengl, F.

Smedes, D. van de Meent, P.J. van den Brink, J. van Gils, A.P. van Wezel, A.D. Vethaak, E. Vermeirssen, P.C. von der Ohe, B. Vrana, Towards the review of the european union water framework management of chemical contamination in european surface water resources, Sci. Total Environ. 576 (2017) 720–737, https://doi.org/10.1016/j.scitotenv.2016.10.104.

[84] C.C. Wu, L.C. Hus, P.N. Chiang, J.C. Liu, W.H. Kuan, C.C. Chen, Y.M. Tzou, M.K. Wang, C.E. Hwang, Oxidative removal of arsenite by Fe(II)- and polyoxometalate (POM)-amended zero-valent aluminum (ZVAl) under oxic conditions, Water Res. 47 (7) (2013) 2583–2591, https://doi.org/10.1016/j.watres.2013.02.024.

[85] Y. Wang, X. Shen, F. Chen, Improving the catalytic activity of CeO2/H2O 2 system by sulfation pretreatment of CeO2, J. Mol. Catal. A Chem. 381 (2014) 38–45, https://doi.org/10.1016/j.molcata.2013.10.003.

[86] A.D. Bokare, W. Choi, Advanced oxidation process based on the Cr(III)/Cr(VI) Redox Cycle, Environ. Sci. Technol. 45 (21) (2011) 9332–9338, https://doi.org/10.1021/es2021704.

[87] Y. Yao, Y. Cai, G. Wu, F. Wei, X. Li, H. Chen, S. Wang, Sulfate radicals induced from peroxymonosulfate by cobalt manganese oxides (CoxMn3-xO4) for fenton-Like reaction in water, J. Hazard. Mater. 296 (2015) 128–137, https://doi.org/10.1016/j.jhazmat.2015.04.014.

[88] Y. Yao, H. Chen, C. Lian, F. Wei, D. Zhang, G. Wu, B. Chen, S. Wang, Fe Co, Ni nanocrystals encapsulated in nitrogen-doped carbon nanotubes as Fenton-like catalysts for organic pollutant removal, J. Hazard. Mater. 314 (2016) 129–139, https://doi.org/10.1016/j.jhazmat.2016.03.089.

[89] A. Hassani, G. Çelikdağ, P. Eghbali, M. Sevim, S. Karaca, Ö. Metin, Heterogeneous sono-Fenton-like process using magnetic cobalt ferrite-reduced graphene oxide (CoFe2O4-rGO) nanocomposite for the removal of organic dyes from aqueous solution, Ultrason. Sonochem. 40 (2018) 841–852, https://doi.org/10.1016/j.ultsonch.2017.08.026.

[90] S. Rahim Pouran, A. Bayrami, A.R. Abdul Aziz, W.M.A. Wan Daud, M.S. Shafeeyan, Ultrasound and UV assisted fenton treatment of recalcitrant wastewaters using transition metal-substituted-magnetite nanoparticles, J. Mol. Liq. 222 (2016) 1076–1084, https://doi.org/10.1016/j.molliq.2016.07.120.

[91] M. Dükkancı, Sono-photo-Fenton oxidation of bisphenol-A over a LaFeO3 perovskite catalyst, Ultrason. Sonochem. 40 (2018) 110–116, https://doi.org/10.1016/j.ultsonch.2017.04.040.

[92] A.J. Expósito, J.M. Monteagudo, A. Durán, A. Fernández, Dynamic behavior of hydroxyl radical in sono-photo-fenton mineralization of synthetic municipal wastewater effluent containing antipyrine, Ultrason. Sonochem. 35 (2017) 185–195, https://doi.org/10.1016/j.ultsonch.2016.09.017.

[93] S. Papoutsakis, S. Miralles-Cuevas, N. Gondrexon, S. Baup, S. Malato, C. Pulgarin, Coupling between high-frequency ultrasound and solar photo-Fenton at pilot scale for the treatment of organic contaminants: An initial approach, Ultrason. Sonochem. 22 (2015) 527–534, https://doi.org/10.1016/j.ultsonch.2014.05.003.

[94] F. Sepyani, R. Darvishi Cheshmeh Soltani, S. Jorfi, H. Godini, M. Safari, Implementation of continuously electro-generated Fe3O4 nanoparticles for activation of persulfate to decompose amoxicillin antibiotic in aquatic media: UV254 and ultrasound intensification, J. Environ. Manage. 224 (2018) 315–326, https://doi.org/10.1016/j.jenvman.2018.07.072.

[95] H. Mostafa, B.M. Iqdiam, M. Abuagela, M.R. Marshall, P. Pullammanappallil, R. Goodrich-Schneider, Treatment of olive mill wastewater using high power ultrasound (hpu) and electro-fenton (EF) method, Chem. Eng. Process. - Process Intensif. 131 (2018) 131–136, https://doi.org/10.1016/j.cep.2018.07.015.

[96] W.S. Chen, Y.C. Jhou, C.P. Huang, Mineralization of dinitrotoluenes in industrial wastewater by electro-activated persulfate oxidation, Chem. Eng. J. 252 (2014) 166–172, https://doi.org/10.1016/j.cej.2014.05.033.

[97] X. Wang, L. Wang, J. Li, J. Qiu, C. Cai, H. Zhang, Degradation of Acid Orange 7 by persulfate activated with zero valent iron in the presence of ultrasonic irradiation, Sep. Purif. Technol. 122 (2014) 41–46, https://doi.org/10.1016/j.seppur.2013.10.037.

[98] H.V. Lutze, N. Kerlin, T.C. Schmidt, Sulfate radical-based water treatment in presence of chloride: Formation of chlorate, inter-conversion of sulfate radicals into hydroxyl radicals and influence of bicarbonate, Water Res. 72 (2015) 349–360, https://doi.org/10.1016/j.watres.2014.10.006.

[99] D.N. Wordofa, S.L. Walker, H. Liu, Sulfate radical-induced disinfection of pathogenic escherichia coli o157:h7 via iron-activated persulfate, Environ. Sci. Technol. Lett. 4 (4) (2017) 154–160, https://doi.org/10.1021/acs.estlett.7b0003510.1021/acs.estlett.7b00035.s001.

[100] Y. Feng, D. Wu, Y.u. Deng, T. Zhang, K. Shih, Sulfate radical-mediated degradation of sulfadiazine by cufeo2 rhombohedral crystal-catalyzed peroxymonosulfate: synergistic effects and mechanisms, Environ. Sci. Technol. 50 (6) (2016) 3119–3127, https://doi.org/10.1021/acs.est.5b0597410.1021/acs.est.5b05974.s001.

[101] N. Yan, F. Liu, W. Huang, Interaction of oxidants in siderite catalyzed hydrogen peroxide and persulfate system using trichloroethylene as a target contaminant, Chem. Eng. J. 219 (2013) 149–154, https://doi.org/10.1016/j.cej.2012.12.072.

[102] N. Yan, F. Liu, Q. Xue, M.L. Brusseau, Y. Liu, J. Wang, Degradation of trichloroethene by siderite-catalyzed hydrogen peroxide and persulfate: Investigation of reaction mechanisms and degradation products, Chem. Eng. J. 274 (2015) 61–68, https://doi.org/10.1016/j.cej.2015.03.056.

[103] L.W. Matzek, K.E. Carter, Activated persulfate for organic chemical degradation: A review, Chemosphere. 151 (2016) 178–188, https://doi.org/10.1016/j.chemosphere.2016.02.055.

[104] B. Li, J. Zhu, Simultaneous degradation of 1,1,1-trichloroethane and solvent stabilizer 1,4-dioxane by a sono-activated persulfate process, Chem. Eng. J. 284 (2016) 750–763, https://doi.org/10.1016/j.cej.2015.08.153.

[105] S. Wang, N. Zhou, Removal of carbamazepine from aqueous solution using sono-activated persulfate process, Ultrason. Sonochem. 29 (2016) 156–162, https://doi.org/10.1016/J.ULTSONCH.2015.09.008.

[106] S. Wang, N. Zhou, S. Wu, Q. Zhang, Z. Yang, Modeling the oxidation kinetics of sono-activated persulfate's process on the degradation of humic acid, Ultrason. Sonochem. 23 (2015) 128–134, https://doi.org/10.1016/j.ultsonch.2014.10.026.

[107] D. Deng, X. Lin, J. Ou, Z. Wang, S. Li, M. Deng, Y. Shu, Efficient chemical oxidation of high levels of soil-sorbed phenanthrene by ultrasound induced, thermally activated persulfate, Chem. Eng. J. 265 (2015) 176–183, https://doi.org/10.1016/j.cej.2014.12.055.

[108] B. Li, L. Li, K. Lin, W. Zhang, S. Lu, Q. Luo, Removal of 1,1,1-trichloroethane from aqueous solution by a sono-activated persulfate process, Ultrason. Sonochem. 20 (3) (2013) 855–863.

[109] E.-T. Yun, H.-Y. Yoo, H. Bae, H.-I. Kim, J. Lee, Exploring the role of persulfate in the activation process: radical precursor versus electron acceptor, Environ. Sci. Technol. 51 (17) (2017) 10090–10099, https://doi.org/10.1021/acs.est.7b0251910.1021/acs.est.7b02519.s001.

[110] C. Zhu, F. Zhu, C. Liu, N. Chen, D. Zhou, G. Fang, J. Gao, Reductive hexachloroethane degradation by s2o8•– with thermal activation of persulfate under anaerobic conditions, Environ. Sci. Technol. 52 (15) (2018) 8548–8557, https://doi.org/10.1021/acs.est.7b0627910.1021/acs.est.7b06279.s001.

[111] S. Giannakis, K.-Y. Lin, F. Ghanbari, A review of the recent advances on the treatment of industrial wastewaters by Sulfate Radical-based Advanced Oxidation Processes (SR-AOPs), Chem. Eng. J. 406 (2021) 127083, https://doi.org/10.1016/j.cej.2020.127083.

[112] S. Luo, Z. Wei, D.D. Dionysiou, R. Spinney, W.P. Hu, L. Chai, Z. Yang, T. Ye, R. Xiao, Mechanistic insight into reactivity of sulfate radical with aromatic contaminants through single-electron transfer pathway, Chem. Eng. J. 327 (2017) 1056–1065, https://doi.org/10.1016/J.CEJ.2017.06.179.

[113] F. Hao, W. Guo, A. Wang, Y. Leng, H. Li, Intensification of sonochemical degradation of ammonium perfluorooctanoate by persulfate oxidant, Ultrason. Sonochem. 21 (2) (2014) 554–558, https://doi.org/10.1016/j.ultsonch.2013.09.016.

[114] X. Zou, T. Zhou, J. Mao, X. Wu, Synergistic degradation of antibiotic sulfadiazine in a heterogeneous ultrasound-enhanced Fe0/persulfate Fenton-like system, Chem. Eng. J. 257 (2014) 36–44, https://doi.org/10.1016/j.cej.2014.07.048.

[115] W.S. Chen, C.P. Huang, Mineralization of dinitrotoluenes in aqueous solution by sono-activated persulfate enhanced with electrolytes, Ultrason. Sonochem. 51 (2019) 129–137, https://doi.org/10.1016/j.ultsonch.2018.10.035.

[116] Z. Wei, F.A. Villamena, L.K. Weavers, Kinetics and mechanism of ultrasonic activation of persulfate: an in situ epr spin trapping study, Environ. Sci. Technol. 51 (6) (2017) 3410–3417, https://doi.org/10.1021/acs.est.6b0539210.1021/acs.est.6b05392.s001.

[117] W.-S. Chen, Y.-C. Su, Removal of dinitrotoluenes in wastewater by sono-activated persulfate, Ultrason. Sonochem. 19 (4) (2012) 921–927.

[118] D.A. House, Kinetics and mechanism of oxidations by peroxydisulfate, Chem. Rev. 62 (3) (1962) 185–203, https://doi.org/10.1021/cr60217a001.

[119] J. Carpenter, M. Badve, S. Rajoriya, S. George, V.K. Saharan, A.B. Pandit, Hydrodynamic cavitation: an emerging technology for the intensification of various chemical and physical processes in a chemical process industry, Rev. Chem. Eng. 33 (2017) 433–468, https://doi.org/10.1515/revce-2016-0032.

[120] Y. Çalışkan, H.C. Yatmaz, N. Bektaş, Photocatalytic oxidation of high concentrated dye solutions enhanced by hydrodynamic cavitation in a pilot reactor, Process Saf. Environ. Prot. 111 (2017) 428–438, https://doi.org/10.1016/j.psep.2017.08.003.

[121] X. Wang, J. Jia, Y. Wang, Degradation of C.I. Reactive Red 2 through photocatalysis coupled with water jet cavitation, J. Hazard. Mater. 185 (1) (2011) 315–321.

[122] M.V. Bagal, P.R. Gogate, Degradation of diclofenac sodium using combined processes based on hydrodynamic cavitation and heterogeneous photocatalysis, Ultrason. Sonochem. 21 (3) (2014) 1035–1043, https://doi.org/10.1016/j.ultsonch.2013.10.020.

[123] G. Li, L. Yi, J. Wang, Y. Song, Hydrodynamic cavitation degradation of rhodamine B assisted by Fe3 + -doped TiO2: Mechanisms, geometric and operation parameters, Ultrason. Sonochem. 60 (2020) 104806, https://doi.org/10.1016/j.ultsonch.2019.104806.

[124] J. Basiri Parsa, S.A. Ebrahimzadeh Zonouzian, Optimization of a heterogeneous catalytic hydrodynamic cavitation reactor performance in decolorization of rhodamine B: Application of scrap iron sheets, Ultrason. Sonochem. 20 (6) (2013) 1442–1449.

[125] Y. Tao, J. Cai, X. Huai, B. Liu, A novel antibiotic wastewater degradation technique combining cavitating jets impingement with multiple synergetic methods, Ultrason. Sonochem. 44 (2018) 36–44, https://doi.org/10.1016/J.ULTSONCH.2018.02.008.

[126] B. Bethi, S.H. Sonawane, G.S. Rohit, C.R. Holkar, D.V. Pinjari, B.A. Bhanvase, A.B. Pandit, Investigation of TiO2 photocatalyst performance for decolorization in the presence of hydrodynamic cavitation as hybrid AOP, Ultrason. Sonochem. 28 (2016) 150–160, https://doi.org/10.1016/J.ULTSONCH.2015.07.008.

[127] P. Li, Y. Song, S. Wang, Z. Tao, S. Yu, Y. Liu, Enhanced decolorization of methyl orange using zero-valent copper nanoparticles under assistance of hydrodynamic cavitation, Ultrason. Sonochem. 22 (2015) 132–138, https://doi.org/10.1016/J.ULTSONCH.2014.05.025.

[128] M.F.R. Samsudin, S. Sufian, B.H. Hameed, Epigrammatic progress and perspective on the photocatalytic properties of BiVO4-based photocatalyst in photocatalytic water treatment technology: A review, J. Mol. Liq. 268 (2018)

438–459, https://doi.org/10.1016/J.MOLLIQ.2018.07.051.
[129] S. Das, A.P. Bhat, P.R. Gogate, Degradation of dyes using hydrodynamic cavitation: Process overview and cost estimation, J. Water Process Eng. 42 (2021) 102126, https://doi.org/10.1016/j.jwpe.2021.102126.
[130] S. Rajoriya, J. Carpenter, V.K. Saharan, A.B. Pandit, Hydrodynamic cavitation: an advanced oxidation process for the degradation of bio-refractory pollutants, Rev. Chem. Eng. 32 (2016) 379–411, https://doi.org/10.1515/revce-2015-0075.
[131] Y. Ku, K.-y. Chen, K.-C. Lee, Ultrasonic destruction of 2-chlorophenol in aqueous solution, Water Res. 31 (4) (1997) 929–935, https://doi.org/10.1016/S0043-1354(96)00372-7.
[132] A. Mirzaei, Z. Chen, F. Haghighat, L. Yerushalmi, Removal of pharmaceuticals from water by homo/heterogonous Fenton-type processes – A review, Chemosphere. 174 (2017) 665–688, https://doi.org/10.1016/j.chemosphere.2017.02.019.
[133] C.-C. Kuan, S.-Y. Chang, S.L.M. Schroeder, Fenton-like oxidation of 4-chlorophenol: homogeneous or heterogeneous? Ind. Eng. Chem. Res. 54 (33) (2015) 8122–8129, https://doi.org/10.1021/acs.iecr.5b02378.
[134] A. Babuponnusami, K. Muthukumar, A review on fenton and improvements to the fenton process for wastewater treatment, J. Environ. Chem. Eng. 2 (1) (2014) 557–572.
[135] B.G. Kwon, D.S. Lee, N. Kang, J. Yoon, Characteristics of p-chlorophenol oxidation by Fenton's reagent, Water Res. 33 (9) (1999) 2110–2118, https://doi.org/10.1016/S0043-1354(98)00428-X.
[136] D.H. Bremner, S.D. Carlo, A.G. Chakinala, G. Cravotto, Mineralisation of 2,4-dichlorophenoxyacetic acid by acoustic or hydrodynamic cavitation in conjunction with the advanced Fenton process, Ultrason. Sonochem. 15 (4) (2008) 416–419, https://doi.org/10.1016/j.ultsonch.2007.06.003.
[137] P.R. Gogate, G.S. Bhosale, Comparison of effectiveness of acoustic and hydrodynamic cavitation in combined treatment schemes for degradation of dye wastewaters, Chem. Eng. Process. Process Intensif. 71 (2013) 59–69, https://doi.org/10.1016/j.cep.2013.03.001.
[138] C. Özdemir, M.K. Öden, S. Şahinkaya, E. Kalipçi, Color removal from synthetic textile wastewater by sono-fenton process, CLEAN – Soil, Air, Water. 39 (1) (2011) 60–67, https://doi.org/10.1002/clen.201000263.
[139] Z. He, S. Song, H. Ying, L. Xu, J. Chen, p-Aminophenol degradation by ozonation combined with sonolysis: Operating conditions influence and mechanism, Ultrason. Sonochem. 14 (5) (2007) 568–574, https://doi.org/10.1016/j.ultsonch.2006.10.002.
[140] A. Fernandes, P. Makoś, G. Boczkaj, Treatment of bitumen post oxidative effluents by sulfate radicals based advanced oxidation processes (S-AOPs) under alkaline pH conditions, J. Clean. Prod. 195 (2018) 374–384, https://doi.org/10.1016/j.jclepro.2018.05.207.
[141] B. Darsinou, Z. Frontistis, M. Antonopoulou, I. Konstantinou, D. Mantzavinos, Sono-activated persulfate oxidation of bisphenol A: Kinetics, pathways and the controversial role of temperature, Chem. Eng. J. 280 (2015) 623–633, https://doi.org/10.1016/J.CEJ.2015.06.061.
[142] Y. Fan, Y. Ji, D. Kong, J. Lu, Q. Zhou, Kinetic and mechanistic investigations of the degradation of sulfamethazine in heat-activated persulfate oxidation process, J. Hazard. Mater. 300 (2015) 39–47, https://doi.org/10.1016/j.jhazmat.2015.06.058.
[143] O.S. Furman, A.L. Teel, R.J. Watts, Mechanism of base activation of persulfate, Environ. Sci. Technol. 44 (16) (2010) 6423–6428, https://doi.org/10.1021/es1013714.
[144] J.M. Monteagudo, H. El-taliawy, A. Durán, G. Caro, K. Bester, Sono-activated persulfate oxidation of diclofenac: Degradation, kinetics, pathway and contribution of the different radicals involved, J. Hazard. Mater. 357 (2018) 457–465, https://doi.org/10.1016/j.jhazmat.2018.06.031.
[145] S. Chakma, S. Praneeth, V.S. Moholkar, Mechanistic investigations in sono-hybrid (ultrasound/Fe2 + /UVC) techniques of persulfate activation for degradation of Azorubine, Ultrason. Sonochem. 38 (2017) 652–663, https://doi.org/10.1016/j.ultsonch.2016.08.015.
[146] H. Kusic, I. Peternel, S. Ukic, N. Koprivanac, T. Bolanca, S. Papic, A.L. Bozic, Modeling of iron activated persulfate oxidation treating reactive azo dye in water matrix, Chem. Eng. J. 172 (1) (2011) 109–121, https://doi.org/10.1016/j.cej.2011.05.076.
[147] H. Ferkous, S. Merouani, O. Hamdaoui, C. Pétrier, Persulfate-enhanced sonochemical degradation of naphthol blue black in water: Evidence of sulfate radical formation, Ultrason. Sonochem. 34 (2017) 580–587, https://doi.org/10.1016/J.ULTSONCH.2016.06.027.
[148] X.J. Zhou, W.Q. Guo, S.S. Yang, H.S. Zheng, N.Q. Ren, Ultrasonic-assisted ozone oxidation process of triphenylmethane dye degradation: Evidence for the promotion effects of ultrasonic on malachite green decolorization and degradation mechanism, Bioresour. Technol. 128 (2013) 827–830, https://doi.org/10.1016/j.biortech.2012.10.086.
[149] C. Pétrier, A. Francony, Ultrasonic waste-water treatment: Incidence of ultrasonic frequency on the rate of phenol and carbon tetrachloride degradation, Ultrason. Sonochem. 4 (4) (1997) 295–300, https://doi.org/10.1016/S1350-4177(97)00036-9.
[150] A. Henglein, C. Kormann, Scavenging of oh radicals produced in the sonolysis of water, Int. J. Radiat. Biol. Relat. Stud. Physics, Chem. Med. 48 (2) (1985) 251–258, https://doi.org/10.1080/09553008514551241.
[151] H.R. Rogers, Sources, behaviour and fate of organic contaminants during sewage treatment and in sewage sludges, Science of The Total Environment 185 (1–3) (1996) 3–26.
[152] Z.-L. Wu, B. Ondruschka, P. Bräutigam, Degradation of chlorocarbons driven by hydrodynamic cavitation, Chem. Eng. Technol. 30 (5) (2007) 642–648, https://doi.org/10.1002/ceat.200600288.
[153] P. Sathishkumar, R.V. Mangalaraja, H.D. Mansilla, M.A. Gracia-Pinilla, S. Anandan, Sonophotocatalytic (42kHz) degradation of Simazine in the presence of Au-TiO2 nanocatalysts, Appl. Catal. B Environ. 160–161 (2014) 692–700, https://doi.org/10.1016/j.apcatb.2014.06.027.
[154] L. Jing, B. Chen, D. Wen, J. Zheng, B. Zhang, Pilot-scale treatment of atrazine production wastewater by UV/O3/ultrasound: Factor effects and system optimization, J. Environ. Manage. 203 (2017) 182–190, https://doi.org/10.1016/j.jenvman.2017.07.027.
[155] P. Thanekar, M. Panda, P.R. Gogate, Degradation of carbamazepine using hydrodynamic cavitation combined with advanced oxidation processes, Ultrason. Sonochem. 40 (2018) 567–576, https://doi.org/10.1016/j.ultsonch.2017.08.001.
[156] D. Musmarra, M. Prisciandaro, M. Capocelli, D. Karatza, P. Iovino, S. Canzano, A. Lancia, Degradation of ibuprofen by hydrodynamic cavitation: Reaction pathways and effect of operational parameters, Ultrason. Sonochem. 29 (2016) 76–83, https://doi.org/10.1016/j.ultsonch.2015.09.002.
[157] E. Nie, M. Yang, D. Wang, X. Yang, X. Luo, Z. Zheng, Degradation of diclofenac by ultrasonic irradiation: Kinetic studies and degradation pathways, Chemosphere. 113 (2014) 165–170, https://doi.org/10.1016/j.chemosphere.2014.05.031.
[158] S.B. Randhavane, A.K. Khambete, Hydrodynamic cavitation: An approach to degrade chlorpyrifos pesticide from real effluent, KSCE J. Civ. Eng. 22 (7) (2018) 2219–2225, https://doi.org/10.1007/s12205-017-2045-0.
[159] R.H. Jawale, P.R. Gogate, A.B. Pandit, Treatment of cyanide containing wastewater using cavitation based approach, Ultrason. Sonochem. 21 (4) (2014) 1392–1399, https://doi.org/10.1016/j.ultsonch.2014.01.025.
[160] C. Wang, Y. Shih, Degradation and detoxification of diazinon by sono-fenton and sono-fenton-like processes, Sep. Purif. Technol. 140 (2015) 6–12, https://doi.org/10.1016/j.seppur.2014.11.005.
[161] P.N. Patil, P.R. Gogate, Degradation of dichlorvos using hybrid advanced oxidation processes based on ultrasound, J. Water Process Eng. 8 (2015) e58–e65, https://doi.org/10.1016/j.jwpe.2014.10.012.
[162] S. Raut-Jadhav, M.P. Badve, D.V. Pinjari, D.R. Saini, S.H. Sonawane, A.B. Pandit, Treatment of the pesticide industry effluent using hydrodynamic cavitation and its combination with process intensifying additives (H2O2 and ozone), Chem. Eng. J. 295 (2016) 326–335, https://doi.org/10.1016/j.cej.2016.03.019.
[163] M. Badve, P. Gogate, A. Pandit, L. Csoka, Hydrodynamic cavitation as a novel approach for wastewater treatment in wood finishing industry, Sep. Purif. Technol. 106 (2013) 15–21, https://doi.org/10.1016/j.seppur.2012.12.029.
[164] A. Montusiewicz, S. Pasieczna-Patkowska, M. Lebiocka, A. Szaja, M. Szymańska-Chargot, Hydrodynamic cavitation of brewery spent grain diluted by wastewater, Chem. Eng. J. 313 (2017) 946–956, https://doi.org/10.1016/j.cej.2016.10.132.
[165] K.V. Padoley, V.K. Saharan, S.N. Mudliar, R.A. Pandey, A.B. Pandit, Cavitationally induced biodegradability enhancement of a distillery wastewater, J. Hazard. Mater. 219–220 (2012) 69–74, https://doi.org/10.1016/j.jhazmat.2012.03.054.
[166] M. Zupanc, T. Kosjek, M. Petkovšek, M. Dular, B. Kompare, B. Širok, M. Stražar, E. Heath, Shear-induced hydrodynamic cavitation as a tool for pharmaceutical micropollutants removal from urban wastewater, Ultrason. Sonochem. 21 (3) (2014) 1213–1221, https://doi.org/10.1016/j.ultsonch.2013.10.025.